

General Disclaimer

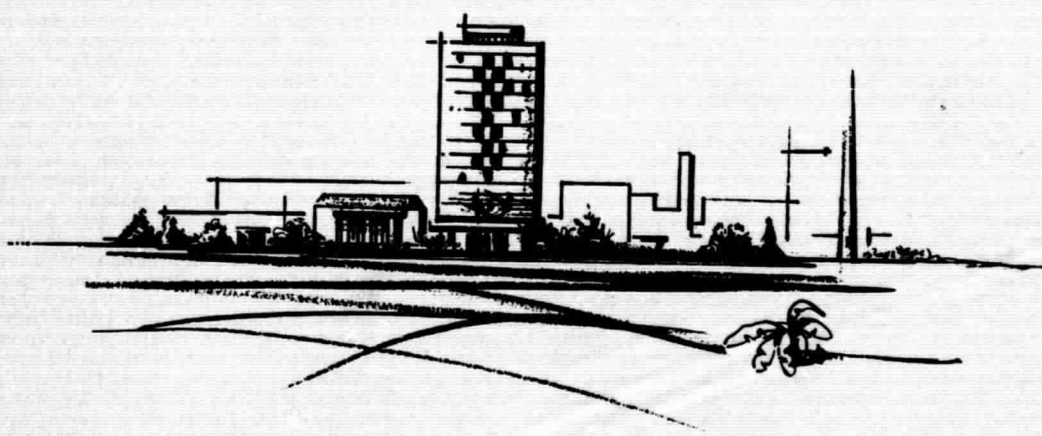
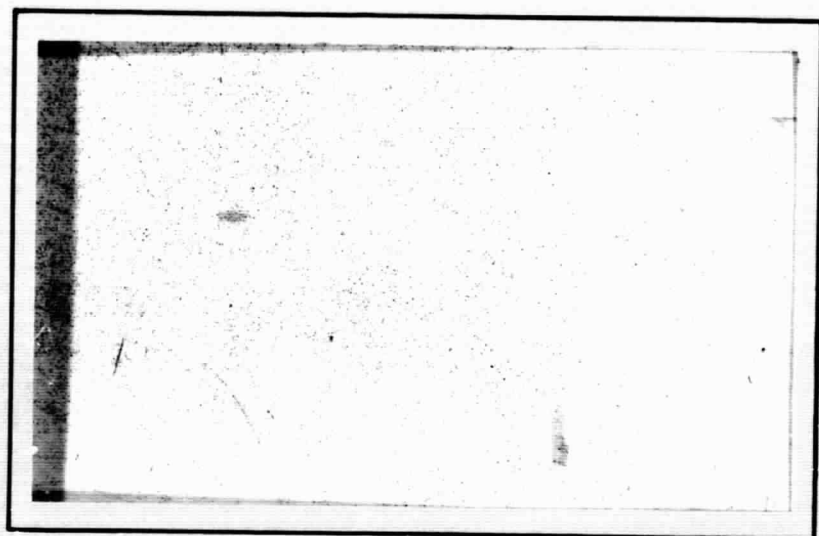
One or more of the Following Statements may affect this Document

- This document has been reproduced from the best copy furnished by the organizational source. It is being released in the interest of making available as much information as possible.
- This document may contain data, which exceeds the sheet parameters. It was furnished in this condition by the organizational source and is the best copy available.
- This document may contain tone-on-tone or color graphs, charts and/or pictures, which have been reproduced in black and white.
- This document is paginated as submitted by the original source.
- Portions of this document are not fully legible due to the historical nature of some of the material. However, it is the best reproduction available from the original submission.

no contact

get DRA

RESEARCH REPORT



BATTELLE MEMORIAL INSTITUTE

COLUMBUS LABORATORIES

FACILITY FORM 602	N71 22527	
	(ACCESSION NUMBER)	(THRU)
	31	63
	(PAGES)	(CODE)
1R-117855		
(NASA CR OR TMX OR AD NUMBER)		
15		
(CATEGORY)		

SUMMARY REPORT

on

ANALYSIS OF BRINELLING FAILURE OF BEARINGS
FROM VIBRATION TESTED PLV FANS

to

NATIONAL AERONAUTICS AND SPACE ADMINISTRATION
GEORGE C. MARSHALL SPACE FLIGHT CENTER

by

W. A. Glaeser, S. K. Batra, and R. H. Prause

June 8, 1970

BATTELLE MEMORIAL INSTITUTE
Columbus Laboratories
505 King Avenue
Columbus, Ohio 43201

TABLE OF CONTENTS

	<u>Page</u>
SUMMARY	1
STATEMENT OF THE PROBLEM	2
THE MODE OF ANALYSIS	2
Analysis of Failed Bearings	2
VIBRATION ANALYSIS	8
Dynamic Analysis Model	9
Experimental Measurements	14
Methods for Modifying Bearing Load Levels	16
Angular Contact Bearing Design Analysis	17
RECOMMENDED PROCEDURE FOR CHOICE OF BEARINGS IN SIMILAR FUTURE APPLICATIONS	31
CONCLUSIONS AND RECOMMENDATIONS FOR FUTURE WORK	33
FUTURE WORK.	33
APPENDIX A	
ANALYSIS OF FAN BEARING LOADS FROM RANDOM VIBRATIONS	A-1
Example Calculation	A-5
APPENDIX B	
ANALYSIS OF THE ANGULAR CONTACT BALL BEARING FOR AXIAL THRUST LOAD	B-1
PROGRAM AXLOD	

SUMMARY REPORT

on

ANALYSIS OF BRINELLING FAILURE OF BEARINGS
FROM VIBRATION TESTED PLV FANS

to

NATIONAL AERONAUTICS AND SPACE ADMINISTRATION

from

BATTELLE MEMORIAL INSTITUTE
Columbus Laboratories

SUMMARY

Brinelling damage has been identified in PLV fan bearings as the cause for noisy running after exposure to a random-vibration environment.

Assuming a maximum Hertz stress of 460,000 psi to produce brinelling, the maximum axial load for the fan bearing was calculated as 43 pounds. Dynamic analysis of the rotor-bearing-spring system revealed that with one preload spring, the maximum predicted axial load would be 297 pounds. Reduction in maximum bearing loads under vibration conditions can be achieved by reducing the rotor natural frequency and by increasing the damping through using a soft spring system. This means multiple springs at both ends of the shaft. When a system of five springs at each end of the rotor was considered, the bearing load predicted was 58 pounds. Actual vibration tests at Marshall Space Flight Center using the 5-spring preload configuration have resulted in reduction of bearing damage. Use of Belleville springs for this particular rotor-bearing configuration was found undesirable because the collapse load of the springs would be easily exceeded during the anticipated operating conditions.

A bearing load-capacity computer program was written so that, given the bearing parameters, inner race diameter, ball diameter, diametral clearance, total curvature of the race groove and number of balls, the limiting axial load can be determined using maximum Hertz stress and over-riding of the race land as the failure criteria.

STATEMENT OF THE PROBLEM

PLV fans subjected to acceptance vibration tests have developed rough running, noisy bearings. Brinelling of the bearing races was suspected as the cause of rough running. If brinelling has been the cause, then overloading of the bearings from inertial loads has occurred and can only be alleviated by increasing the size of the bearing or reducing the peak inertial loads. If fretting or "false brinelling" has been the cause of rough races, then load capacity of the bearing will have no significance in the severity of the effect. Brinelling is a plastic deformation process; fretting is a time-dependent wear process and the latter is a function of rubbing amplitude and lubrication.

THE MODE OF ANALYSIS

An analysis was performed on the rotor-bearing system to determine the following:

- (1) The nature of damage to fan bearings (whether it is brinelling or fretting).
- (2) The maximum bearing loads resulting from test random vibration environment.
- (3) Hertz stresses developed in the bearings and displacement of balls in races using the load values obtained in Number (2).
- (4) The influence of bearing preload and preload spring configuration on bearing contact stress levels.

Analysis of Failed Bearings

Samples of both new bearings and bearings from noisy fans were analyzed in the Battelle Lubrication Mechanics Laboratory. Bearings were disassembled and the race surfaces examined by stereoptican microscope. The race surface topography was measured with a Talyrond roundness instrument.

Microscopy revealed classic brinelling on the inner and outer races of bearings taken from tested fans. The following bearings were examined:

- (1) Used bearing with much of the grease gone. Severe brinelling over-running the lip of the ball groove. brinelling on one side of the race groove.

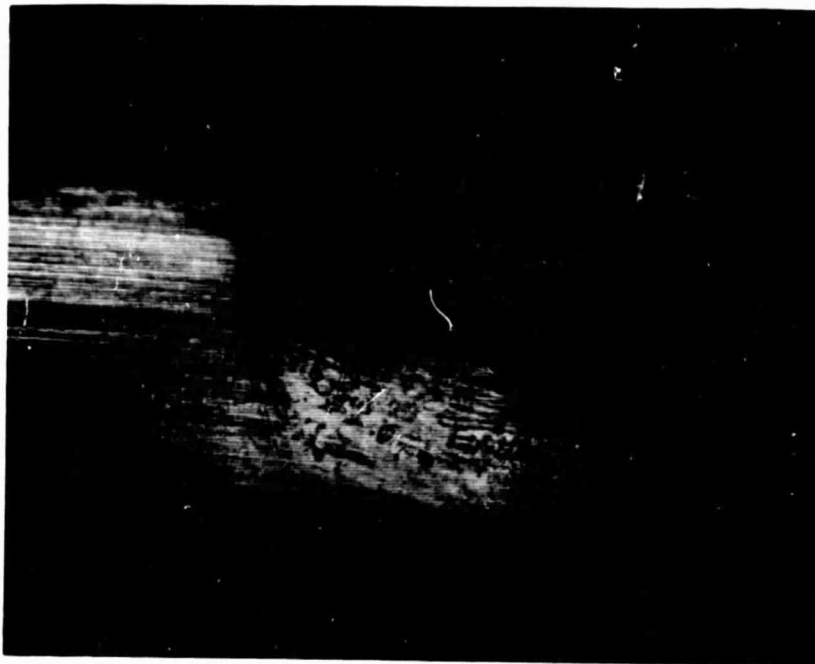
- (2) New bearing filled with grease. All surfaces free of defects.
- (3) Used bearing with much of the grease gone. Mild brinelling on inner and outer races.
- (4) Used bearing with some residual grease. One set of brinell marks on inner race and barely visible on outer race.
- (5) Used bearing full of grease. Very light brinell marks on inner and outer races.

The extent of ball indentation in the severely brinelled bearing is shown in the photomicrograph in Figure 1.

Talyrond measurements were made on several circumferential positions of the inner races of the bearings. The traces were made with the stylus riding (1) on the bottom of the ball groove, (2) on the side of the ball groove, and (3) on the race lands. Typical traces of brinelled bearings are shown in Figures 2, 3, and 4. The location of the tracing stylus is shown in the drawing at the top of each tracing. For instance, the trace in Figure 2a was made on the race land.

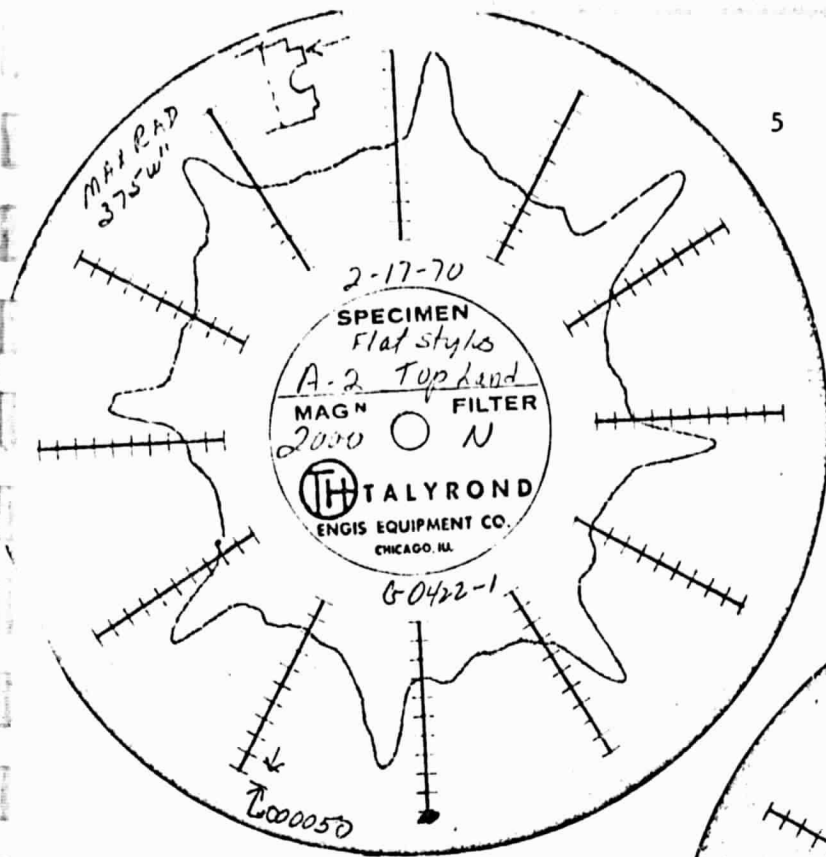
Figure 2 shows an example of heavy brinelling. The bearing was so overloaded axially that the balls were driven up the sides of the ball groove and indented the lip causing a mounding up on the race land surface. The mounding up can be seen in Figure 2a. Each mound represents the position of one ball in the bearing. All eight balls have produced indentations. The height of the mounds averaged 0.00025 inch. The indentations in the thrust side of the ball groove can be seen in Figure 3. The trace indicates one set of severe brinell marks together with at least two other sets of lighter brinell marks. Apparently this bearing was subjected to several separate conditions of axial vibration, one of them being most severe. Average depth of the severe indentations was about 0.00025 inch. Width of the indentations at the surface averaged about 0.03 inch. (The proportions of the indentations are distorted on the Talyrond traces because radial magnification is much higher than circumferential.)

The brinell marks did not extend into the bottom of the race groove as shown in the trace in Figure 2b. The trace is smooth, and slightly egg-shaped,

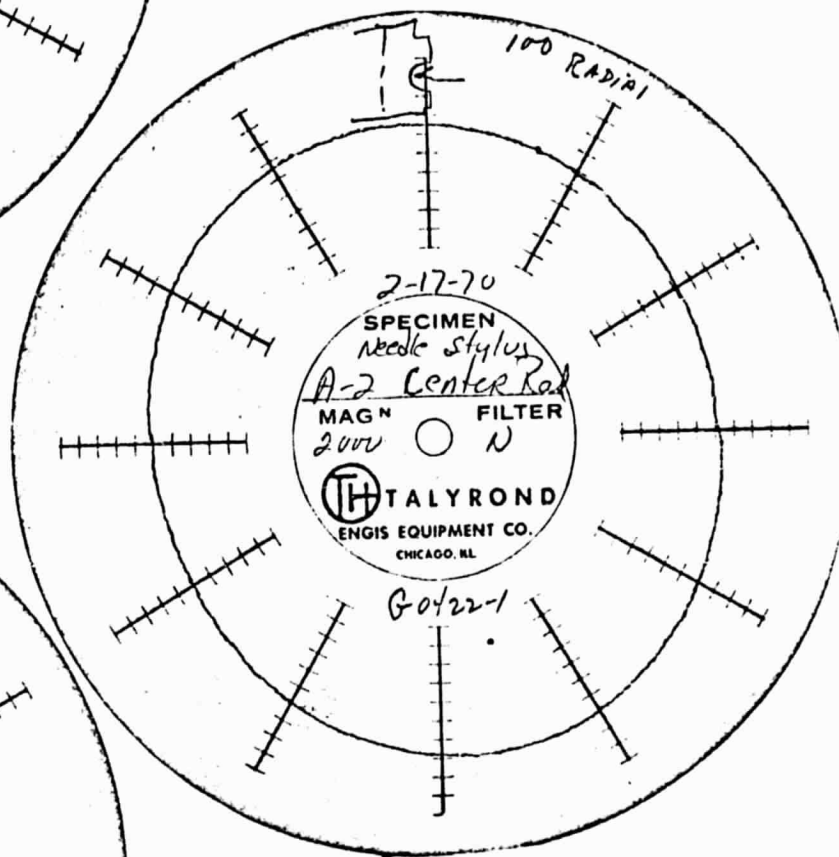


75 X

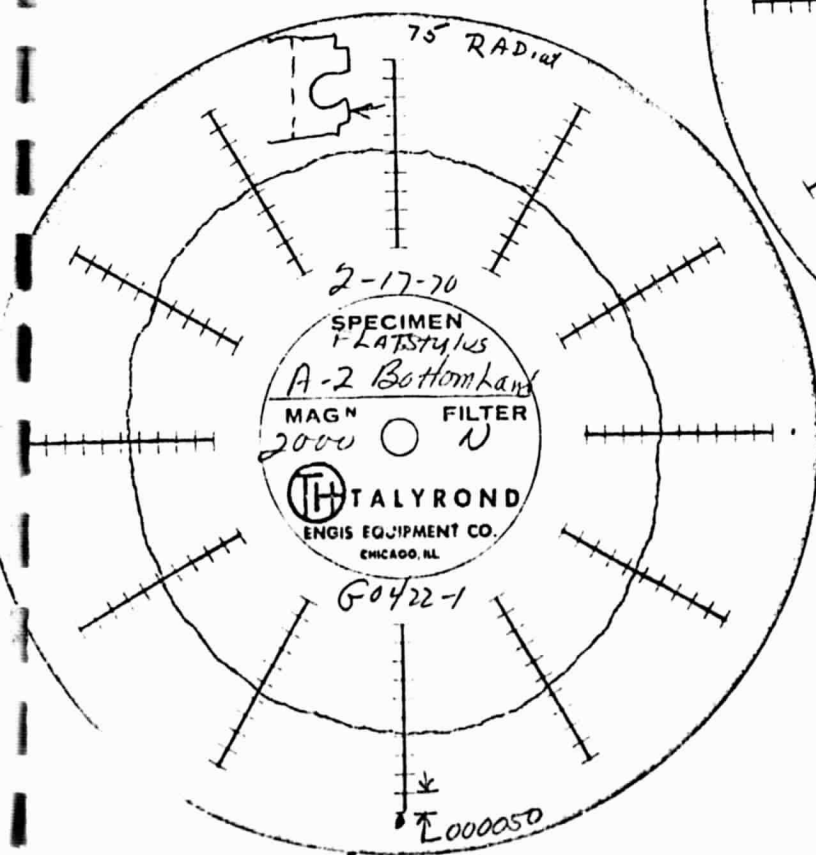
FIGURE 1. SEVERE BRINELLING DAMAGE ON INNER RACE OF FAN BEARING. THE PHOTOGRAPH SHOWS ONE BALL INDENTATION EXTENDING OVER THE RACE GROOVE LIP



a. Land surface



b. Bottom of race groove



c. Land surface

FIGURE 2. TALLYROND TRACES OF SEVERELY BRINELLED FAN BEARING INNER RACE

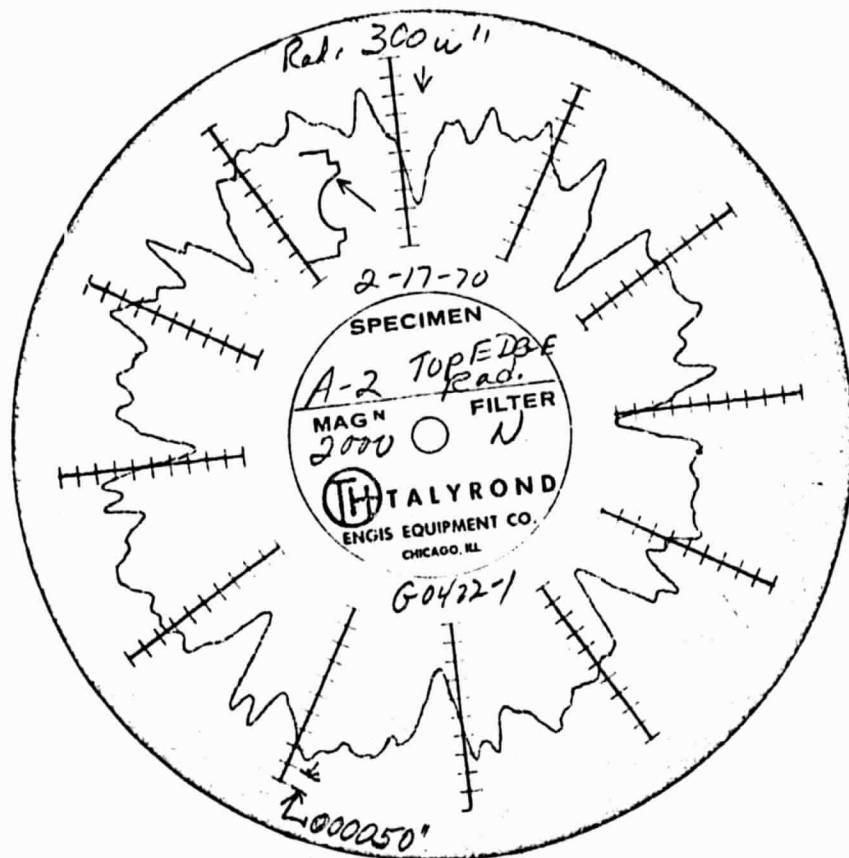
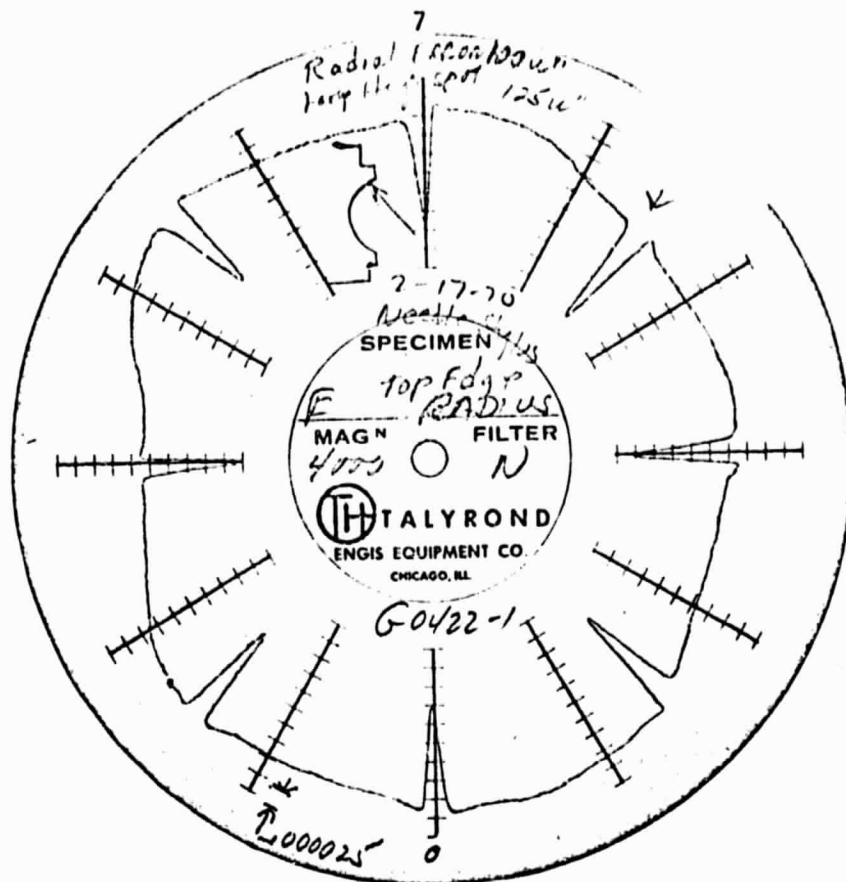
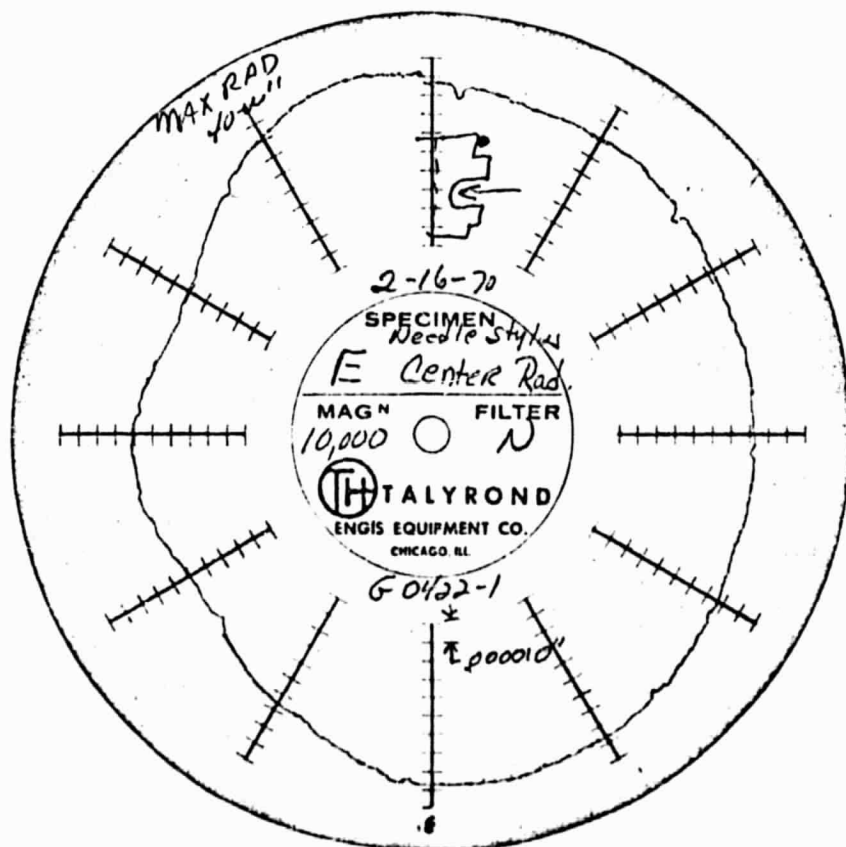


FIGURE 3. TALYROND TRACE OF SEVERELY BRINELLED FAN BEARING INNER RACE TAKEN ON THE THRUST SIDE OF THE RACE GROOVE



a. Thrust side of race groove



b. Bottom of race groove

FIGURE 4. TALYROND TRACES OF LIGHTLY BRINELLED FAN BEARING INNER RACE

indicating ovality in the race geometry. It was concluded, therefore, that brinelling damage was associated with axial loads and not radial loads.

An example of light brinelling damage is shown in Figure 4. These marks were barely visible under the microscope. Maximum depth of the indentations are about 0.0001 inch. Note that faint indications of light dents show up in the trace made of the bottom of the ball groove. This indicates that the balls were not displaced as far from their no-load position as they were in the bearing exhibiting heavy brinelling. In addition, the trace shows only one set of brinell marks in this bearing. If the bearing was subjected to more than one vibration condition only one was severe enough to produce damage.

It has been concluded from the examination of failed bearings that the damage is true brinelling resulting from inertial overloads and that the conformity and radial play conditions in these bearings allow sufficient relative motion of rolling elements under axial load so that ball over-riding of the race groove lip is possible under heavy enough load.

VIBRATION ANALYSIS

An important objective of this program was to establish an analytical method for estimating maximum bearing loads when the PLV fan was subjected to a random vibration environment. Calculated bearing loads could then be used to compare the predicted results with the experience from tests where bearings have failed, and to evaluate proposed modifications to the bearing support system in order to select a modification most promising for further testing.

Equations for predicting the maximum expected rotor displacements and bearing loads have been derived and a detailed development is included in Appendix A, with numerical examples to demonstrate correct application. These equations are based on certain simplifying assumptions regarding the shape of the power spectrum of the vibration test specifications, as well as the use of a linear spring representation for the shaft bearings and preload springs, which are actually quite nonlinear. Even so, it is believed that this idealized model is a useful design tool.

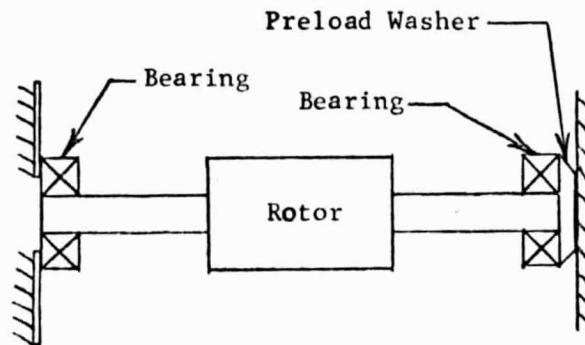
Dynamic Analysis Model

Figure 5a is a sketch of the original configuration of the fan rotor and bearings¹ using one wave washer to obtain a 6 pounds axial preload. Figure 5b shows springs representing the flexibility of the bearings and preload washer, and this is transformed to the equivalent single-degree-of-freedom model shown in Figure 5c. The washer is very flexible relative to the bearings. Therefore, the only contribution of the washer is to establish sufficient preload so that for small motions about the shaft equilibrium position, the total effective stiffness is that of the one bearing that is preloaded against the rigid housing.

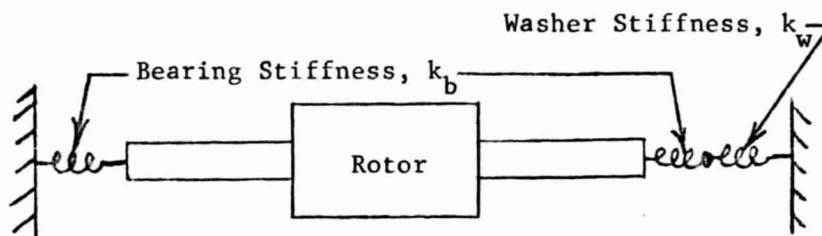
When the shaft deflection exceeds the 0.005 inch preload deflection, the bearing will be unloaded, and the effective stiffness will be that of the wave washer. Figure 6 shows the load-deflection curves for several different preloads to demonstrate how the bearing stiffness is the important parameter in determining the effective axial stiffness. These curves also show the net external force limitations imposed by the 43 pounds maximum axial load capability of the bearings. There will be no significant change in these curves if multiple washers are used to replace the single washer so long as they are all on one end of the shaft and the total preload force is the same.

If, however, washers are installed at both ends of the shaft, Figure 7 shows that the stiffness of the flexible washers will be the determining factor of the total effective stiffness. Figure 8 shows several load-deflection curves for five Belleville springs stacked in parallel at each end of the shaft. The load-deflection characteristics obtained from MSFC Drawing SK20-5072 indicate these springs have a maximum load capability of about 14.5 pounds and Figure 8 shows this collapse load.

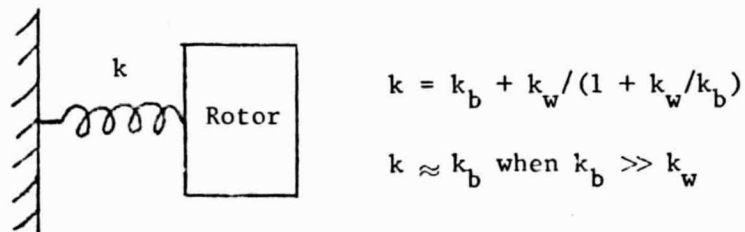
¹ The bearing considered in the analysis was Barden SR4SS, One-quarter-inch bore, angular contact, currently in use. Assuming a limiting maximum Hertz stress of 460,000 psi, the maximum axial load capacity of the bearing was determined as 43 pounds using the computer program described in the next section.



a. Bearing Support Configuration



b. Spring Model of Bearing Supports



c. Simplified Model for Dynamic Analysis

FIGURE 5. DEVELOPMENT OF MODEL REPRESENTING THE AXIAL DYNAMICS OF THE PLV FAN ROTOR ASSEMBLY WHEN PRELOADED BY FLEXIBLE WASHERS AT ONE END

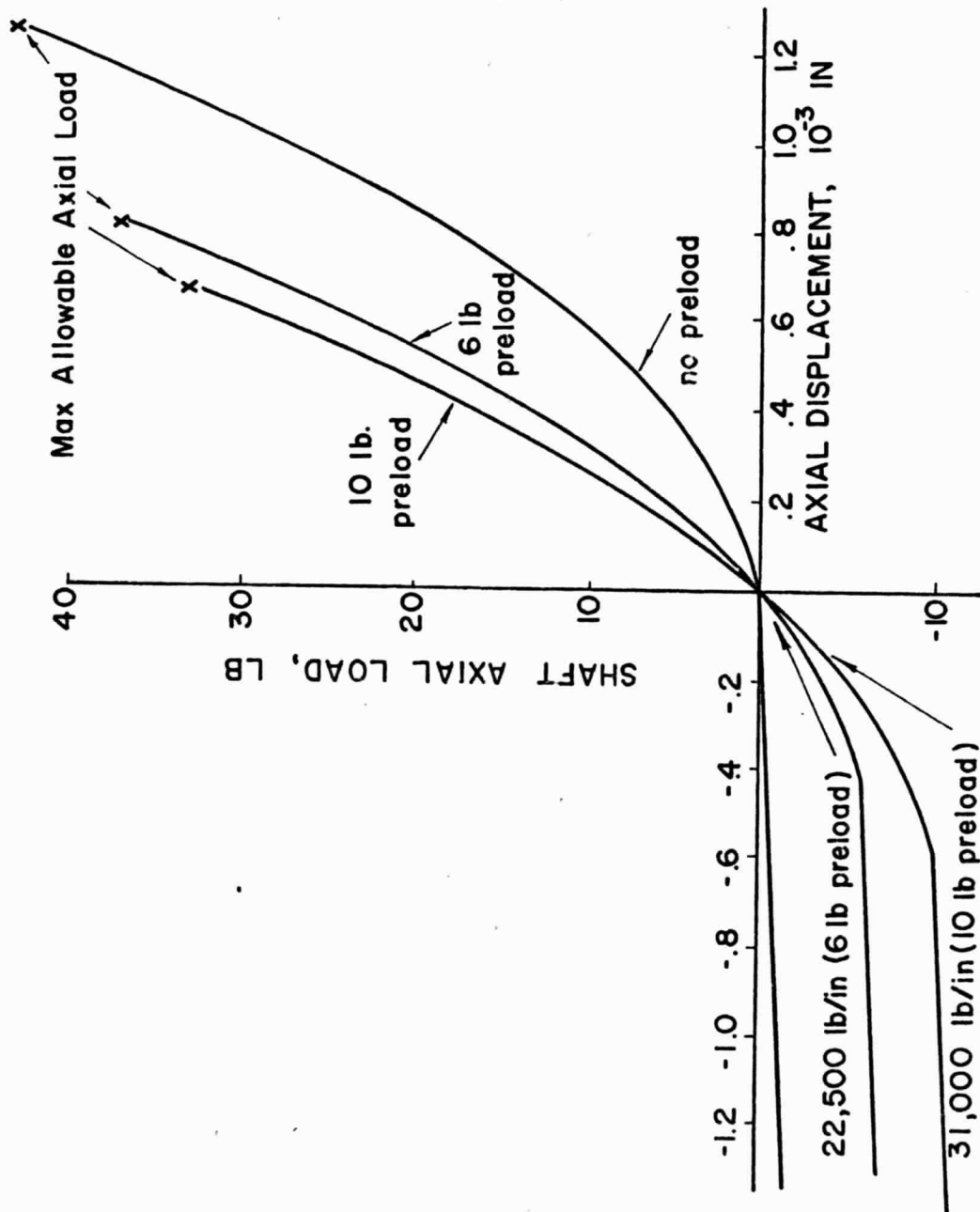
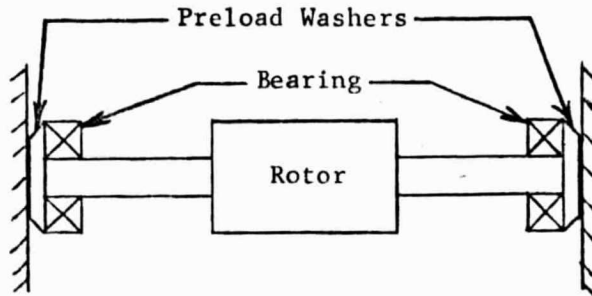
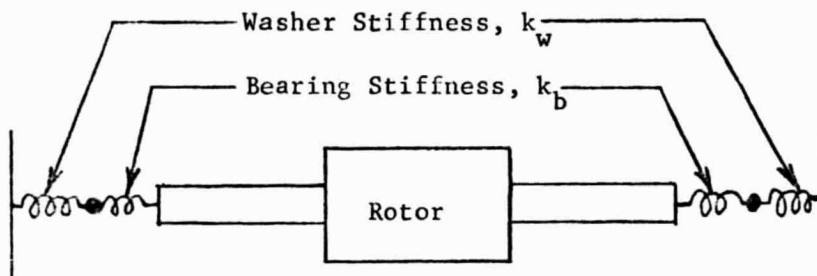


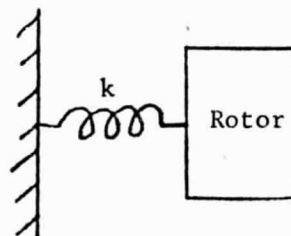
FIGURE 6. AXIAL LOAD-DEFLECTION CURVES FOR FAN SHAFT
PRELOADED BY ONE WAVE WASHER AT ONE END



a. Bearing Support Configuration



b. Spring Model of Bearing Supports



$$k = 2k_w / (1 + k_w/k_b)$$

$$k \approx 2k_w \text{ when } k_b \gg k_w$$

c. Simplified Model for Dynamic Analysis

FIGURE 7. DEVELOPMENT OF MODEL REPRESENTING THE AXIAL DYNAMICS OF THE PLV FAN ROTOR ASSEMBLY WHEN PRELOADED BY FLEXIBLE WASHERS AT BOTH ENDS

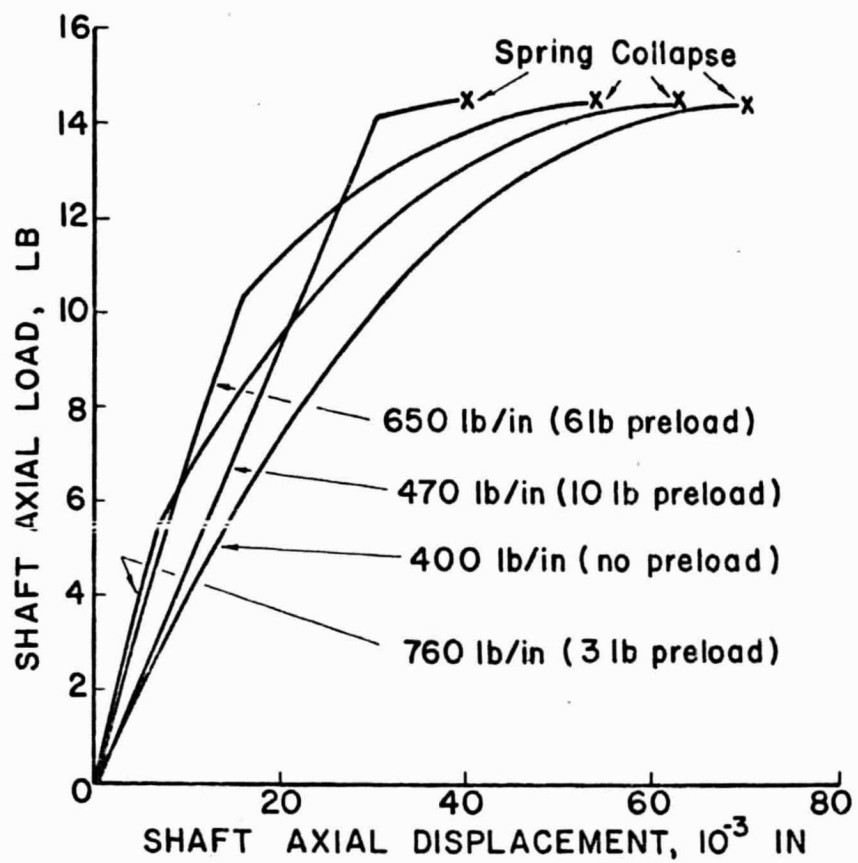


FIGURE 8. AXIAL LOAD-DEFLECTION CURVES FOR FAN SHAFT WITH FIVE BELLEVILLE SPRINGS AT EACH END STACKED IN PARALLEL

Experimental Measurements

In order to predict the maximum expected bearing loads using the equations derived in Appendix A, it is necessary to know the natural frequency and the resonant amplification factor Q of the rotor in the axial direction. The natural frequency can be predicted analytically, at least within the linear system approximations, but the Q of the system must be measured.

In order to measure both the natural frequency and effective damping (Q), the fan housing was clamped rigidly in a heavy vise and a soft rubber mallet was used to tap the rotor and produce a transient vibration. A Kistler Model 802-A piezoelectric accelerometer mounted on the fan impeller was used with a Kistler Model 568 charge amplifier, and the vibration signal was displayed on a Tektronix Type 502 oscilloscope. A Polaroid camera was used to record the transient vibration and the photographs were analyzed to determine the natural frequency and damping.

Table 1 summarizes the measured frequencies and Q factors for three bearing support configurations. Equations A-13 and A-15 in Appendix A were used to calculate the maximum expected bearing loads and rotor displacements. Although the calculated values of bearing loads for the original fan configuration (Configuration I) are probably higher than would be actually measured because of the neglected nonlinearities, it is evident that the bearing loads from the vibration tests are considerably higher than the 43 pounds maximum allowable load. The observed reduction in natural frequency at higher vibration amplitudes was caused by the rotor motion exceeding the washer preload so that the bearings were unloaded for part of each vibration cycle. The photographs of the transient vibration indicated that the preload was exceeded at an amplitude of about 0.004 inches (± 16 g's), which agrees closely with the design specifications for the wave washer.

With one Belleville spring installed at each end of the shaft, the calculated and measured natural frequencies were in close agreement and the damping was increased considerably (lower Q). However, the vibration environment is most severe in the frequency range of 60 to 150 Hz (see Figure A-2) so the predicted bearing loads are excessive and the Belleville springs would collapse.

TABLE 1. SUMMARY OF MEASURED ROTOR DYNAMIC CHARACTERISTICS AND PREDICTED BEARING LOADS FOR 100 PERCENT LEVEL VIBRATION TEST SPECIFICATIONS

Configuration	Rotor Natural Frequency, Hz		Q	Maximum Predicted	
	Theoretical	Measured		Bearing Load, lb (3)	Rotor Displacement, inch
I. One Wave Washer at one end 6 lb design preload	427(4)	494(+10 g's) 440(+20 g's) 385(+80 g's)	44 24	297(1) 205(1)	0.0099 0.0087
II. One Belleville Spring each end Approximately 10 lb preload	138	125	11	118(1,2)	0.123
III. Five Belleville Springs each end Approximately 6 lb preload	73	100	3	58(1,2)	0.090

- (1) Exceeds maximum allowable bearing load.
(2) Exceeds Belleville spring collapse load.
(3) 100 percent Level Vibration Test Specification (MSFC Memo. S&E-ASTN-EME-69-243).
(4) A 10 lb preload gives a 500 Hz theoretical natural frequency.

With five Belleville springs at each end (Configuration 3) the damping was increased considerably. The predicted loads were reduced sufficiently to suggest that the bearings might be capable of surviving the vibration tests, but the Belleville springs would be expected to collapse. It does not appear practical to use Belleville springs with a 14.5 pounds collapse load with bearings which have a 43 pounds allowable load.

Methods for Modifying Bearing Load Levels

Figure A-2 shows that the most severe vibration excitation is in the 60-540 Hz frequency range with reduced levels extending to the 20 Hz low frequency limit and to the 2000 Hz high frequency limit. In order to reduce the fan bearing loads it is obvious from Figure A-2 that to have reduced exciting forces either the natural frequency should be reduced considerably from the 494 Hz resonance of the original design configuration, or the system should be stiffened to increase its natural frequency. One advantage of reducing the natural frequency by supporting the rotor with flexible springs is that this type of modification will increase the damping and reduce the resonant amplification factor Q . If the natural frequency is increased, the damping will be quite low (high Q) as indicated by the measurements, and it is quite difficult to introduce additional damping in a high frequency system.

If it is assumed that $Q = 5$ is reasonable for a softly-sprung bearing mount, the maximum allowable bearing load of 43 pounds can be used to calculate a reasonable frequency suitable for a design goal. Results of this calculation show that the rotor axial natural frequency must be reduced below 55 Hz for the predicted bearing loads to be less than the maximum allowable. For a safety factor of 2, the natural frequency should be below 43 Hz, and the springs must permit the maximum expected rotor displacement of ± 0.19 inch.

These large relative displacements present practical problems because the radial clearance between the bearing O.D. and the bearing housing should be kept small for satisfactory fan operation. However, the bearings must be quite free axially to obtain the required low natural frequency and large displacements. Slight misalignment or excessive friction could bind the bearings so that while a "soft" support system appears theoretically satisfactory, extreme care in manufacturing and assembly would be required to obtain high reliability using the current blaring mount configuration.

The alternative solution of rigidly mounting the bearings to obtain a high natural frequency eliminates the requirement of providing the axial motion. However, it would probably be necessary to increase both the bearing size and number of bearings. For example, if the highest measured value of $Q = 44$ is assumed, the natural frequency must be greater than 2000 Hz if the load on a single bearing is reduced below 43 pounds. If a pair of larger preloaded bearings are used with the rating of each bearing doubled to 86 pounds and the bearing stiffness is increased proportionately (actually the bearing stiffness may increase by a greater factor than the load rating), then the rotor natural frequency would be doubled (≈ 1000 Hz). The total predicted bearing force would be 164 pounds or 82 pounds per bearing, which would be acceptable. The maximum rotor displacement would be only 0.0013 inch. The limitation with this solution is that the bearing housing structure must be rigid relative to the bearings, and it is difficult to design a bearing system that will actually have a resonance as high as 1000 Hz without a severe weight penalty.

After examining the alternatives of either a soft, low-frequency bearing system or a stiff, high-frequency system, it does not appear that the present PLV fan configuration can be easily modified in order to pass the vibration tests and operate reliably. It is recommended that if the fan design is revised, the bearings should be soft-mounted in the axial direction with the flexible element attached rigidly to the bearing outer case to eliminate any sliding elements. Damping should either be obtained with the flexible element, such as the hysteresis loss in an elastomer, or a damping device introducing friction could be attached independent of the bearing supports.

Angular Contact Bearing Design Analysis

Essential features of the angular contact bearing design are reasonably well understood. The mathematical analysis of the geometrical parameters influencing the load capacity of the bearing is well detailed in the books by Harris² and Jones³. In estimating the load capacity of the bearing in the axial and/or radial direction the hydrodynamic effects of lubrication

² Tedric A. Harris, "Rolling Bearing Analysis", 1966, John Wiley & Sons, Inc.

³ A. B. Jones, "Analysis of Stresses and Deflection", Volume 1 and 2, Copyright 1946, New Departure, Division of General Motors Corp.

are generally ignored; the design criteria are based on the Hertz theory of dry-static contact between the rolling elements.

The formulations pertaining to thrust load, applied to single row angular contact bearing, have been employed in the analysis of the PLV for bearings. The appropriate mathematical equations have been adopted from Harris's book. Using these expressions a computer code was written for the G.E. Time Sharing System (Mark I); this is included and explained in Appendix B. This program was written with the intent of providing a useful tool for analyzing the influence of various geometric parameters on the load-deflection curve of PLV fan bearing. For instance for the bearings currently in use, assuming 57 percent conformity and diametral clearance of 0.00065 inch the value of the axial deflections were computed (computer output I) for various static loads.⁴ The load deflection curve is plotted in Figure 9; this curve was used in the dynamic analysis of the previous section.

To illustrate the use of the computer program several additional runs (computer outputs II-V) were made in which ball race conformity and the diametral clearance (contact angle)⁵ were selectively varied. To understand the output of the program reference may be made to the illustration in Figure 10. Here α designates the contact angle and θ_o (θ_i for the inner race) is the minimum angle the outer race must subtend, as shown, in order to avoid the riding of the ball over the land. H_o (H_i for the inner race) designates the minimum land height the outer race must possess in order to prevent ball over riding. All this is true for a given thrust load. The program computes these quantities as well as the maximum Hertz stress for both the inner and

⁴ The critical dimensions used in the analysis for the SR4SS bearing are as follows:

inner race diameter, d_i = 0.3401 inch (See Figure 10)
 ball diameter, D = 0.0937 inch
 number of balls = 8
 diametral clearance = 0.00065 inch
 B, or $(f_i + f_o - 1)$ = 0.14
 where f_i = inner race conformity
 f_o = outer race conformity

⁵ Diametral clearance and contact angle are related in the following way:

$$\alpha = \cos^{-1} \left(\frac{P_d}{2A} \right) \quad \text{where} \quad \begin{array}{ll} \alpha = \text{contact angle} & A = B \times \text{ball diameter} \\ P_d = \text{diametral clearance} & B = f_o + f_i - 1 \end{array}$$

where f_o = outer race groove radius/ ball diameter
 f_i = inner race groove radius/ball diameter.

COMPUTER OUTPUT I

IN PART2

PLV BEARING MAXIMUM LOAD CAPACITY

? 0.34075, 0.09375, 0.00065, 0.148, 0.00453, 460000.

INN. RACE DIA., BALL DIA., DIA. CLEARANCE, B, NO. OF BALLS AND INCREMENT
IN ALFA

.3401	.0937	6.5000E-04	.14	8
.0046				

SM, ARJ 2.862 523222.75

THRUST LOAD, AXL. DSPL.

	RACE , HERTZ	PRESSURE, MIN.	ANGLE	AND LAND HEIGHT
.2352	6.17033E-05			
	INNER	.9401E+05	.2682E+00	.3352E-02
	OUTER	.7788E+05	.2664E+00	.3307E-02
.3363	1.23538E-04			
	INNER	.1337E+06	.2910E+00	.3913E-02
	OUTER	.1108E+06	.2874E+00	.3845E-02
1.592	1.85506E-04			
	INNER	.1646E+06	.3079E+00	.4410E-02
	OUTER	.1364E+06	.3043E+00	.4321E-02
2.5385	2.47612E-04			
	INNER	.1911E+06	.3240E+00	.4878E-02
	OUTER	.1583E+06	.3203E+00	.4769E-02
3.6725	3.09857E-04			
	INNER	.2148E+06	.3339E+00	.5331E-02
	OUTER	.1780E+06	.3347E+00	.5203E-02
4.9951	3.72246E-04			
	INNER	.2366E+06	.3529E+00	.5777E-02
	OUTER	.1960E+06	.3483E+00	.5631E-02
6.51	4.34782E-04			
	INNER	.2569E+06	.3663E+00	.6219E-02
	OUTER	.2129E+06	.3614E+00	.6055E-02
8.2224	4.97466E-04			
	INNER	.2761E+06	.3792E+00	.6661E-02
	OUTER	.2238E+06	.3739E+00	.6478E-02
10.1383	5.60304E-04			
	INNER	.2944E+06	.3918E+00	.7103E-02
	OUTER	.2439E+06	.3861E+00	.6901E-02
12.2649	6.23297E-04			
	INNER	.3120E+06	.4040E+00	.7547E-02
	OUTER	.2584E+06	.3930E+00	.7327E-02
14.6098	6.86450E-04			
	INNER	.3289E+06	.4159E+00	.7994E-02
	OUTER	.2725E+06	.4096E+00	.7755E-02
17.181	7.49765E-04			
	INNER	.3453E+06	.4277E+00	.8444E-02
	OUTER	.2860E+06	.4210E+00	.8187E-02
19.9871	8.13246E-04			
	INNER	.3612E+06	.4392E+00	.8899E-02
	OUTER	.2992E+06	.4323E+00	.8623E-02

COMPUTER OUTPUT I (CONTINUED)

23.1371	8.76396E-04			
	INNER	.3767E+06	.4506E+00	.9358E-02
	OUTER	.3121E+06	.4433E+00	.9063E-02
26.3412	9.40718E-04			
	INNER	.3919E+06	.4619E+00	.9822E-02
	OUTER	.3247E+06	.4543E+00	.9508E-02
29.9161	.001			
	INNER	.4068E+06	.4730E+00	.1029E-01
	OUTER	.3370E+06	.4651E+00	.9958E-02
33.7447	.0011			
	INNER	.4214E+06	.4840E+00	.1077E-01
	OUTER	.3491E+06	.4758E+00	.1041E-01
37.3662	.0011			
	INNER	.4353E+06	.4949E+00	.1125E-01
	OUTER	.3610E+06	.4864E+00	.1087E-01
42.1313	.0012			
	INNER	.4500E+06	.5057E+00	.1173E-01
	OUTER	.3723E+06	.4969E+00	.1134E-01
47.0000	.0013			
	INNER	.4639E+06	.5164E+00	.1222E-01

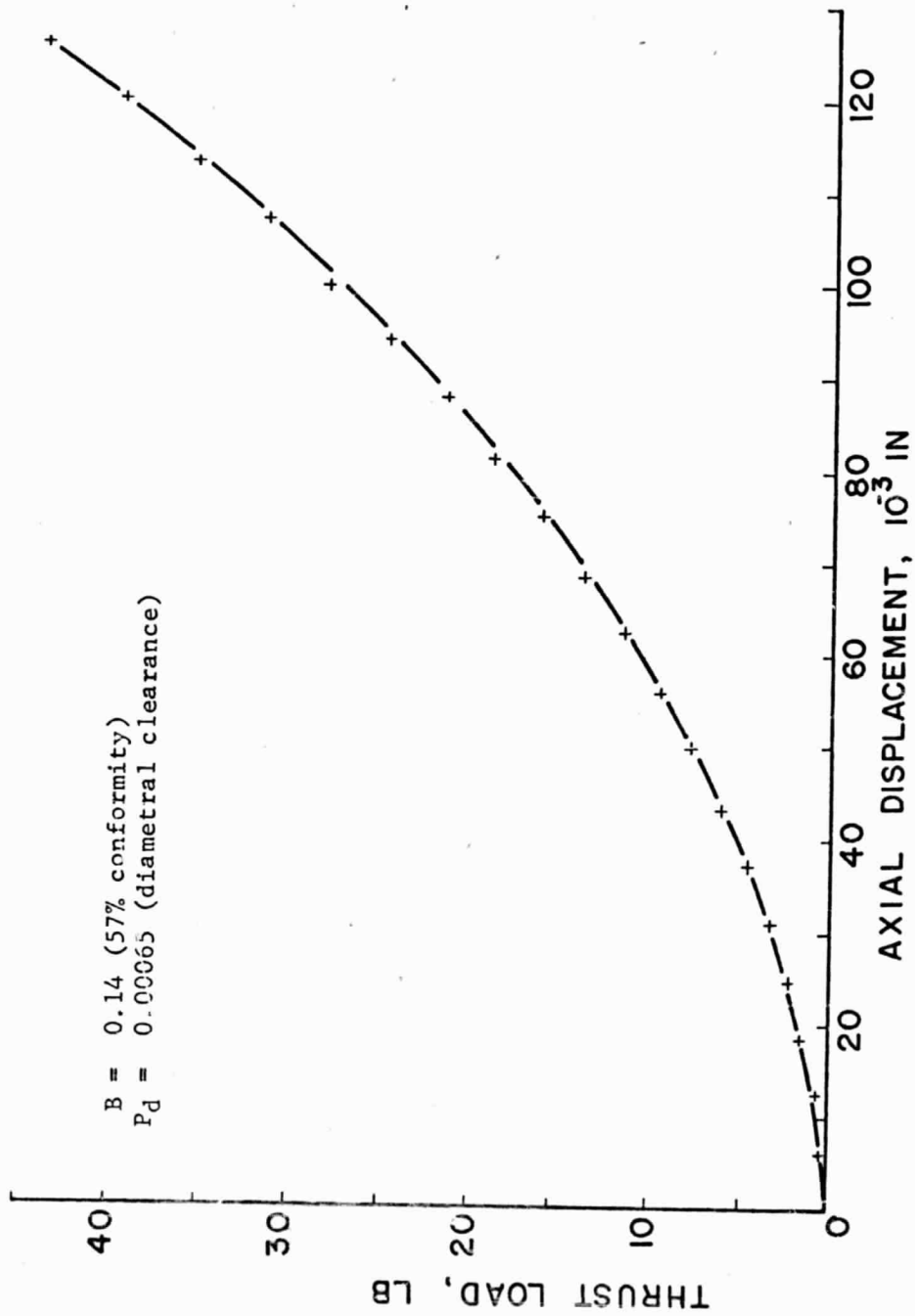


FIGURE 9. LOAD DEFLECTION CURVE FOR PLV FAN BEARING

COMPUTER OUTPUT II

AXL0D 16:07 CY FRI 04/24/70

IN PART2

? 0.340075, 0.09375, 0.0001, 0.04, 8, 0.0046, 460000.

INN. RACE DIA., BALL DIA., DIA. CLEARANCE, B, NO. OF BALLS AND INCREMENT
IN ALFA, MAX HERTZ LIMIT

.3401 .0937 1.00000E-04 .04 8
.0046 460000.00

SM, ABJ 2.1909 120441.83

THRUST LOAD, AKL. DSFL.

	RACE	HERTZ	PRESSURE	MIN.	ANGLE	AND	LAND	HEIGHT
.0303	1.74965E-05							
	INNER	.3812E+05	.2026E+00	.1918E-02				
	OUTER	.3123E+05	.2015E+00	.1896E-02				
.2792	7.01533E-05							
	INNER	.7790E+05	.2525E+00	.2972E-02				
	OUTER	.6382E+05	.2501E+00	.2917E-02				
.7392	1.23078E-04							
	INNER	.1052E+06	.2911E+00	.3944E-02				
	OUTER	.8619E+05	.2879E+00	.3858E-02				
1.4336	1.76293E-04							
	INNER	.1283E+06	.3259E+00	.4935E-02				
	OUTER	.1051E+06	.3220E+00	.4818E-02				
2.3985	2.29821E-04							
	INNER	.1491E+06	.3588E+00	.5969E-02				
	OUTER	.1222E+06	.3542E+00	.5819E-02				
3.6761	2.83686E-04							
	INNER	.1686E+06	.3904E+00	.7053E-02				
	OUTER	.1381E+06	.3852E+00	.6869E-02				
5.3131	3.37912E-04							
	INNER	.1871E+06	.4212E+00	.8193E-02				
	OUTER	.1533E+06	.4154E+00	.7974E-02				
7.3607	3.92522E-04							
	INNER	.2050E+06	.4514E+00	.9391E-02				
	OUTER	.1680E+06	.4451E+00	.9134E-02				
9.8737	4.47542E-04							
	INNER	.2224E+06	.4813E+00	.1065E-01				
	OUTER	.1822E+06	.4744E+00	.1035E-01				
12.9116	5.02998E-04							
	INNER	.2394E+06	.5108E+00	.1197E-01				
	OUTER	.1961E+06	.5034E+00	.1163E-01				

COMPUTER OUTPUT II (CONTINUED)

14.0517	5.21585E-04			
	INNER	.2450E+06	.5206E+00	.1242E-01
	OUTER	.2007E+06	.5130E+00	.1207E-01
15.2595	5.40224E-04			
	INNER	.2506E+06	.5304E+00	.1288E-01
	OUTER	.2053E+06	.5226E+00	.1251E-01
16.5377	5.58917E-04			
	INNER	.2562E+06	.5402E+00	.1335E-01
	OUTER	.2099E+06	.5322E+00	.1297E-01
20.8201	6.15326E-04			
	INNER	.2727E+06	.5694E+00	.1479E-01
	OUTER	.2234E+06	.5609E+00	.1436E-01
25.8313	6.72252E-04			
	INNER	.2891E+06	.5985E+00	.1630E-01
	OUTER	.2368E+06	.5895E+00	.1582E-01
31.6488	7.29726E-04			
	INNER	.3053E+06	.6276E+00	.1787E-01
	OUTER	.2501E+06	.6180E+00	.1734E-01
38.3552	7.87778E-04			
	INNER	.3215E+06	.6567E+00	.1950E-01
	OUTER	.2634E+06	.6465E+00	.1892E-01
46.0354	8.46438E-04			
	INNER	.3376E+06	.6858E+00	.2120E-01
	OUTER	.2766E+06	.6751E+00	.2056E-01
54.792	9.05739E-04			
	INNER	.3537E+06	.7150E+00	.2296E-01
	OUTER	.2898E+06	.7036E+00	.2227E-01
64.7157	9.65715E-04			
	INNER	.3698E+06	.7442E+00	.2478E-01
	OUTER	.3030E+06	.7323E+00	.2403E-01
75.9155	.001			
	INNER	.3859E+06	.7735E+00	.2667E-01
	OUTER	.3162E+06	.7610E+00	.2586E-01
88.5039	.0011			
	INNER	.4020E+06	.8029E+00	.2863E-01
	OUTER	.3294E+06	.7898E+00	.2775E-01
102.6009	.0012			
	INNER	.4182E+06	.8325E+00	.3065E-01

USED 60.00 UNITS

COMPUTER OUTPUT III

INN. RACE DIA., BALL DIA., DIA. CLEARANCE, B, NO. OF BALLS AND INCREMENT I
N ALFA, MAX HERTZ LIMIT

.3401 .0937 1.00000E-04 .1178 8
.0046 460000.00

SM, ABJ 2.7668 428927.06

THRUST LOAD, AXL. DSPL.

RACE, HERTZ PRESSURE, MIN, ANGLE AND LAND HEIGHT

.0287	5.10551E-05			
	INNER	.5543E+05	.1263E+00	.7465E-03
	OUTER	.4583E+05	.1252E+00	.7333E-03
.0879	1.02157E-04			
	INNER	.7933E+05	.1423E+00	.9477E-03
	OUTER	.6559E+05	.1407E+00	.9263E-03
.1746	1.53309E-04			
	INNER	.9829E+05	.1560E+00	.1138E-02
	OUTER	.8126E+05	.1540E+00	.1109E-02
.2898	2.04512E-04			
	INNER	.1148E+06	.1685E+00	.1327E-02
	OUTER	.9490E+05	.1661E+00	.1291E-02
.4356	2.55768E-04			
	INNER	.1298E+06	.1802E+00	.1519E-02
	OUTER	.1073E+06	.1776E+00	.1475E-02
.6146	3.07081E-04			
	INNER	.1437E+06	.1915E+00	.1714E-02
	OUTER	.1188E+06	.1886E+00	.1662E-02
.8295	3.58452E-04			
	INNER	.1569E+06	.2024E+00	.1914E-02
	OUTER	.1297E+06	.1992E+00	.1855E-02
1.0833	4.09884E-04			
	INNER	.1695E+06	.2131E+00	.2120E-02
	OUTER	.1401E+06	.2096E+00	.2052E-02
1.3793	4.61378E-04			
	INNER	.1816E+06	.2235E+00	.2332E-02
	OUTER	.1502E+06	.2198E+00	.2255E-02
1.7209	5.12938E-04			
	INNER	.1934E+06	.2337E+00	.2549E-02
	OUTER	.1599E+06	.2298E+00	.2464E-02
2.1115	5.64565E-04			
	INNER	.2049E+06	.2438E+00	.2773E-02
	OUTER	.1694E+06	.2397E+00	.2679E-02
2.5548	6.16262E-04			
	INNER	.2161E+06	.2538E+00	.3004E-02
	OUTER	.1786E+06	.2494E+00	.2901E-02
3.0546	6.68031E-04			
	INNER	.2271E+06	.2637E+00	.3241E-02
	OUTER	.1877E+06	.2591E+00	.3128E-02
3.6148	7.19874E-04			
	INNER	.2379E+06	.2735E+00	.3484E-02
	OUTER	.1967E+06	.2686E+00	.3362E-02
4.2397	7.71794E-04			
	INNER	.2485E+06	.2832E+00	.3735E-02
	OUTER	.2055E+06	.2781E+00	.3603E-02
4.9333	8.23794E-04			
	INNER	.2590E+06	.2929E+00	.3992E-02
	OUTER	.2141E+06	.2876E+00	.3849E-02
5.70	8.75875E-04			
	INNER	.2694E+06	.3025E+00	.4256E-02
	OUTER	.2227E+06	.2969E+00	.4103E-02

COMPUTER OUTPUT III (CONTINUED)

6.5445	9.28040E-04			
	INNER	.2796E+06	.3120E+00	.4526E-02
	OUTER	.2312E+06	.3063E+00	.4363E-02
7.4712	9.80292E-04			
	INNER	.2898E+06	.3215E+00	.4804E-02
	OUTER	.2396E+06	.3156E+00	.4629E-02
8.485	.001			
	INNER	.2999E+06	.3310E+00	.5089E-02
	OUTER	.2480E+06	.3248E+00	.4903E-02
9.5909	.0011			
	INNER	.3099E+06	.3404E+00	.5330E-02
	OUTER	.2562E+06	.3341E+00	.5182E-02
10.7939	.0011			
	INNER	.3199E+06	.3498E+00	.5678E-02
	OUTER	.2645E+06	.3433E+00	.5469E-02
12.0993	.0012			
	INNER	.3297E+06	.3592E+00	.5984E-02
	OUTER	.2726E+06	.3524E+00	.5762E-02
13.5124	.0012			
	INNER	.3396E+06	.3686E+00	.6296E-02
	OUTER	.2808E+06	.3616E+00	.6062E-02
15.0388	.0013			
	INNER	.3494E+06	.3779E+00	.6615E-02
	OUTER	.2888E+06	.3707E+00	.6368E-02
16.6841	.0013			
	INNER	.3591E+06	.3872E+00	.6942E-02
	OUTER	.2969E+06	.3798E+00	.6682E-02
18.4542	.0014			
	INNER	.3688E+06	.3965E+00	.7275E-02
	OUTER	.3049E+06	.3889E+00	.7002E-02
20.355	.0015			
	INNER	.3785E+06	.4058E+00	.7615E-02
	OUTER	.3129E+06	.3980E+00	.7328E-02
22.3927	.0015			
	INNER	.3881E+06	.4151E+00	.7962E-02
	OUTER	.3209E+06	.4071E+00	.7662E-02
24.5735	.0016			
	INNER	.3977E+06	.4244E+00	.8317E-02
	OUTER	.3288E+06	.4162E+00	.8002E-02
26.9041	.0016			
	INNER	.4073E+06	.4337E+00	.8678E-02
	OUTER	.3367E+06	.4252E+00	.8349E-02
29.3903	.0017			
	INNER	.4169E+06	.4429E+00	.9047E-02
	OUTER	.3447E+06	.4343E+00	.8703E-02
32.0407	.0017			
	INNER	.4264E+06	.4522E+00	.9422E-02
	OUTER	.3525E+06	.4433E+00	.9063E-02
34.8605	.0018			
	INNER	.4359E+06	.4614E+00	.9805E-02
	OUTER	.3604E+06	.4524E+00	.9430E-02
37.8574	.0018			
	INNER	.4454E+06	.4707E+00	.1019E-01
	OUTER	.3683E+06	.4614E+00	.9804E-02
41.0388	.0019			
	INNER	.4549E+06	.4799E+00	.1059E-01
	OUTER	.3761E+06	.4705E+00	.1018E-01
44.412	.0019			
	INNER	.4644E+06	.4892E+00	.1099E-01

COMPUTER OUTPUT IV

INN. RACE DIA., BALL DIA., DIA. CLEARANCE, B, NO. OF BALLS AND INCREMENT
IN ALFA, MAX HERTZ LIMIT

.3401 .0937 8.00000E-04 .04 8
.0046 460000.00

SM, ABJ 2.191 120439.37

THRUST LOAD, AXL. DSFL.

RACE, HERTZ PRESSURE, MIN, ANGLE AND LAND HEIGHT

.4319	1.93546E-05			
	INNER	.6632E+05	.5303E+00	.1290E-01
	OUTER	.5434E+05	.5288E+00	.1280E-01
1.2455	3.88001E-05			
	INNER	.9412E+05	.5606E+00	.1435E-01
	OUTER	.7711E+05	.5578E+00	.1421E-01
2.3326	5.83378E-05			
	INNER	.1157E+06	.5848E+00	.1558E-01
	OUTER	.9477E+05	.5813E+00	.1540E-01
3.6605	7.79693E-05			
	INNER	.1340E+06	.6061E+00	.1670E-01
	OUTER	.1098E+06	.6021E+00	.1648E-01
5.214	9.76961E-05			
	INNER	.1504E+06	.6257E+00	.1776E-01
	OUTER	.1232E+06	.6211E+00	.1751E-01
6.9849	1.17520E-04			
	INNER	.1653E+06	.6439E+00	.1877E-01
	OUTER	.1354E+06	.6388E+00	.1849E-01
8.9692	1.37442E-04			
	INNER	.1791E+06	.6612E+00	.1976E-01
	OUTER	.1468E+06	.6557E+00	.1944E-01
11.1656	1.57464E-04			
	INNER	.1922E+06	.6778E+00	.2072E-01
	OUTER	.1574E+06	.6719E+00	.2038E-01
13.574	1.77537E-04			
	INNER	.2045E+06	.6938E+00	.2167E-01
	OUTER	.1676E+06	.6875E+00	.2129E-01
16.1959	1.97814E-04			
	INNER	.2163E+06	.7093E+00	.2261E-01
	OUTER	.1772E+06	.7026E+00	.2220E-01
19.0335	2.18146E-04			
	INNER	.2277E+06	.7243E+00	.2354E-01
	OUTER	.1865E+06	.7173E+00	.2310E-01
22.0396	2.38584E-04			
	INNER	.2386E+06	.7391E+00	.2446E-01
	OUTER	.1955E+06	.7317E+00	.2399E-01
25.3679	2.59130E-04			
	INNER	.2492E+06	.7535E+00	.2538E-01
	OUTER	.2042E+06	.7458E+00	.2488E-01
28.8722	2.79787E-04			
	INNER	.2595E+06	.7677E+00	.2630E-01
	OUTER	.2126E+06	.7596E+00	.2577E-01
32.6069	3.00555E-04			
	INNER	.2696E+06	.7817E+00	.2721E-01
	OUTER	.2209E+06	.7732E+00	.2666E-01
36.5766	3.21437E-04			
	INNER	.2794E+06	.7954E+00	.2813E-01
	OUTER	.2289E+06	.7867E+00	.2754E-01
40.7866	3.42434E-04			
	INNER	.2889E+06	.8090E+00	.2904E-01
	OUTER	.2368E+06	.8000E+00	.2843E-01
45.2419	3.63549E-04			
	INNER	.2984E+06	.8225E+00	.2996E-01
	OUTER	.2445E+06	.8131E+00	.2930E-01

COMPUTER OUTPUT IV (CONTINUED)

49.9483	3.84782E-04			
	INNER	.3076E+06	.8358E+00	.3088E-01
	OUTER	.2520E+06	.8261E+00	.3021E-01
54.9115	4.06137E-04			
	INNER	.3167E+06	.8489E+00	.3180E-01
	OUTER	.2595E+06	.8389E+00	.3110E-01
60.1376	4.27615E-04			
	INNER	.3256E+06	.8620E+00	.3273E-01
	OUTER	.2668E+06	.8517E+00	.3200E-01
65.6329	4.49217E-04			
	INNER	.3344E+06	.8750E+00	.3366E-01
	OUTER	.2740E+06	.8644E+00	.3289E-01
71.4039	4.70947E-04			
	INNER	.3432E+06	.8879E+00	.3459E-01
	OUTER	.2812E+06	.8769E+00	.3380E-01
77.4574	4.92806E-04			
	INNER	.3518E+06	.9007E+00	.3552E-01
	OUTER	.2882E+06	.8894E+00	.3470E-01
83.8003	5.14795E-04			
	INNER	.3603E+06	.9134E+00	.3646E-01
	OUTER	.2952E+06	.9019E+00	.3561E-01
90.4398	5.36919E-04			
	INNER	.3687E+06	.9261E+00	.3741E-01
	OUTER	.3021E+06	.9142E+00	.3653E-01
97.3331	5.59177E-04			
	INNER	.3770E+06	.9387E+00	.3836E-01
	OUTER	.3089E+06	.9266E+00	.3744E-01
104.638	5.81573E-04			
	INNER	.3853E+06	.9513E+00	.3931E-01
	OUTER	.3157E+06	.9388E+00	.3837E-01
112.2121	6.04109E-04			
	INNER	.3935E+06	.9638E+00	.4027E-01
	OUTER	.3224E+06	.9510E+00	.3930E-01
120.1135	6.26787E-04			
	INNER	.4016E+06	.9763E+00	.4124E-01
	OUTER	.3290E+06	.9632E+00	.4023E-01
128.3505	6.49610E-04			
	INNER	.4097E+06	.9887E+00	.4221E-01
	OUTER	.3357E+06	.9754E+00	.4117E-01
136.9313	6.72579E-04			
	INNER	.4177E+06	.1001E+01	.4319E-01
	OUTER	.3422E+06	.9875E+00	.4212E-01
145.8647	6.95698E-04			
	INNER	.4256E+06	.1014E+01	.4417E-01
	OUTER	.3488E+06	.9996E+00	.4307E-01
155.1595	7.18908E-04			
	INNER	.4336E+06	.1026E+01	.4516E-01
	OUTER	.3552E+06	.1012E+01	.4402E-01
164.8249	7.42393E-04			
	INNER	.4415E+06	.1038E+01	.4616E-01
	OUTER	.3617E+06	.1024E+01	.4499E-01
174.8701	7.65974E-04			
	INNER	.4493E+06	.1051E+01	.4716E-01
	OUTER	.3681E+06	.1036E+01	.4596E-01
185.3047	7.89714E-04			
	INNER	.4571E+06	.1063E+01	.4817E-01
	OUTER	.3745E+06	.1048E+01	.4693E-01
196.1385	8.13617E-04			
	INNER	.4649E+06	.1075E+01	.4918E-01

COMPUTER OUTPUT V

AXL0D 15:27 CY FRI 04/24/70

IN PART2

? 0.340075, 0.09375, 0.00080, 0.1178, 8, 0.0046

? 460000.

INN. RACE DIA., BALL DIA., DIA. CLEARANCE, B, NO. OF BALLS AND INCREMENT
IN ALFA

.3401	.0937	8.00000E-04	.1178	8
.0046				

SM, ABJ 2.7669 428916.72

THRUST LOAD, AXL. DSPL.

	RACE , HERTZ	PRESSURE, MAX.	ANGLE	AND LAND HEIGHT
.3767	5.27779E-05			
	INNER	.9367E+05	.3193E+00	.4740E-02
	OUTER	.7746E+05	.3174E+00	.4684E-02
1.0984	1.05693E-04			
	INNER	.1331E+06	.3428E+00	.5455E-02
	OUTER	.1101E+06	.3401E+00	.5370E-02
2.0796	1.58747E-04			
	INNER	.1638E+06	.3621E+00	.6080E-02
	OUTER	.1354E+06	.3588E+00	.5969E-02
3.2984	2.11945E-04			
	INNER	.1900E+06	.3793E+00	.6663E-02
	OUTER	.1571E+06	.3754E+00	.6529E-02
4.7473	2.65287E-04			
	INNER	.2134E+06	.3951E+00	.7224E-02
	OUTER	.1765E+06	.3908E+00	.7067E-02
6.4246	3.18778E-04			
	INNER	.2349E+06	.4100E+00	.7772E-02
	OUTER	.1942E+06	.4052E+00	.7593E-02
8.3323	3.72420E-04			
	INNER	.2549E+06	.4243E+00	.8312E-02
	OUTER	.2108E+06	.4191E+00	.8112E-02
10.4741	4.26216E-04			
	INNER	.2738E+06	.4380E+00	.8848E-02
	OUTER	.2264E+06	.4323E+00	.8626E-02
12.8552	4.80169E-04			
	INNER	.2917E+06	.4512E+00	.9382E-02
	OUTER	.2412E+06	.4452E+00	.9139E-02

COMPUTER OUTPUT V (CONTINUED)

15.4818	5.34282E-04			
	INNER	.3089E+06	.4641E+00	.9917E-02
	OUTER	.2554E+06	.4573E+00	.9652E-02
18.361	5.88558E-04			
	INNER	.3255E+06	.4767E+00	.1045E-01
	OUTER	.2691E+06	.4700E+00	.1017E-01
21.5004	6.43000E-04			
	INNER	.3415E+06	.4891E+00	.1099E-01
	OUTER	.2824E+06	.4820E+00	.1068E-01
24.9231	6.97611E-04			
	INNER	.3570E+06	.5012E+00	.1153E-01
	OUTER	.2952E+06	.4938E+00	.1120E-01
28.5927	7.52394E-04			
	INNER	.3722E+06	.5131E+00	.1207E-01
	OUTER	.3077E+06	.5055E+00	.1172E-01
32.5632	8.07353E-04			
	INNER	.3869E+06	.5249E+00	.1262E-01
	OUTER	.3200E+06	.5169E+00	.1225E-01
36.8271	8.62490E-04			
	INNER	.4014E+06	.5366E+00	.1317E-01
	OUTER	.3319E+06	.5283E+00	.1278E-01
41.40	9.17809E-04			
	INNER	.4156E+06	.5481E+00	.1373E-01
	OUTER	.3437E+06	.5395E+00	.1331E-01
46.2861	9.73313E-04			
	INNER	.4295E+06	.5595E+00	.1429E-01
	OUTER	.3552E+06	.5506E+00	.1385E-01
51.4977	.001			
	INNER	.4433E+06	.5703E+00	.1486E-01
	OUTER	.3665E+06	.5616E+00	.1440E-01
57.0454	.0011			
	INNER	.4568E+06	.5820E+00	.1543E-01
	OUTER	.3777E+06	.5725E+00	.1495E-01
62.9403	.0011			
	INNER	.4701E+06	.5931E+00	.1601E-01

outer race, at the specified increments in α . It continues to do so until the maximum Hertz pressure at the inner race (or outer race) exceeds the limiting value specified through input, at which point it terminates further calculations. The termination of calculations is also affected if the required value of θ_0 (or θ_1) exceeds $\pi/2$.

In the computer output II and III it may be observed that for a limiting Hertz stress of 460,000 psi the load capacity of the bearing is reduced from approximately 102 pounds to 44 pounds as the parameter B, or $(f_o + f_i - 1)$ is increased from 0.04 to 0.1178, keeping all other geometrical parameters constant. Increasing B reduces ball-race conformity or the closeness of fit between ball and race groove.

Computer outputs IV and V for the same calculations are repeated for an 8-fold increase in diametral clearance. These results indicate that the reduction in conformity level (or increase in B) reduces the load carrying capacity of the bearing, whereas an increase in diametral clearance (which increases contact angle) increases the load capacity with a limit imposed by race land height. Thus, by changing the contact angle with the present size bearing, an increase in load capacity is possible without changing bearing size. It must be kept in mind, however, that increasing contact angle will also increase ball spin and heat generation in the bearing. This effect will tend to reduce the endurance life of the bearing in terms of lubricant degradation and ball wear.

RECOMMENDED PROCEDURE FOR CHOICE OF BEARINGS IN SIMILAR FUTURE APPLICATIONS

The analysis of the present PLV fan bearings has demonstrated the importance of the dynamical considerations in the choice of bearings for a similar application. At the same time, one is forced to recognize that it is not possible to outline a simple step-by-step procedure that would end in the selection of a bearing satisfying all the design requirements. As is typical of such problems the designer must consider the influence of various parameters on the outcome before arriving at the final optimum design. The next few paragraphs present a plan of analysis to arrive at such an optimum design.

It is assumed that the mass of the rotor is known. It is also assumed that Power Spectral Density (PSD) of the vibration environment to be imposed on the rotor, is known. It is desired to determine the maximum axial load that would be borne by the bearing under fairly severe conditions. Based on this estimate, the geometry of the angular contact bearing would be selected so as to avoid the brinelling of the race as well as balls over-riding the race land. To facilitate the choice of the bearing it is necessary that this load-limit be as small as possible.

Equation (A-14) relates the axial load on the bearing with the stiffness of the system, its damping, and the maximum expected amplitude of vibration on the bearing-rotor assembly. The expected amplitude of vibration, for the white-noise approximation, is in turn related to the maximum value of the PSD (W_0) resonant frequency (f_n) and the magnification factor (Q) as given by (A-13). If the axial displacement of the rotor must be kept at an absolute minimum (from the viewpoint of design limitation) then the resonant frequency of the system must be chosen past the higher end of the PSD spectrum to minimize the value of W_0 . This requires that stiffness of the system be high which would in turn require that the support system must be made very rigid. The latter requirement may be difficult to realize if the stipulated resonant frequency is of the order of 2000 HZ and over; in this case a compromise will have to be made, such as, allowing for larger amplitude-limit and perhaps even larger loads on the bearing. If, however, the required resonant frequency can be obtained with a reasonably rigid support system the reduction of the load-limit on the bearing would be easily achieved in the high-frequency end of the PSD spectrum.

On the other hand, if the axial displacement is not the limiting quantity, the load-limit on the bearing can be reduced by going to the low-frequency-end of the PSD spectrum. Below a certain level of the resonant frequency the value of W_0 will decrease. The low resonant frequency can be designed by suspending the rotor-bearing system in a soft suspension system (e.g. five springs in the present PLV fan bearings) such that the preloaded bearing acts essentially as a rigid member. For the suspension system use can be made of thick elastomeric packing material which would provide high damping factor as well. It is, of course, necessary that the "collapse-

load" of the soft suspension system be at least as high as the maximum load capacity of the bearing.

Once the load limit of the bearing has been arrived at, in the above manner, the design parameter for the angular contact bearing can be established by the computer program described in the preceding section. To guard against brinelling it is recommended that maximum Hertz pressure be kept below 460,000 psi under all conditions. This would then provide a limiting criteria for the geometrical parameters of the bearings to be selected.

CONCLUSIONS AND RECOMMENDATIONS FOR FUTURE WORK

The following conclusions have been drawn from the analysis of the PLV fan bearing problem:

- (1) The bearing failure mode is vibration induced race brinelling, the damaging loads occurring in the axial direction.
- (2) Maximum bearing load can be reduced by decreasing the natural frequency of the rotor-bearing-preload spring system. This can be accomplished by mounting preload springs in series at both bearing supports on the rotor.
- (3) A computer program, written to calculate maximum load capacity based on brinelling mode of failure, has demonstrated that bearing load capacity can be increased by altering contact angle and ball-race conformity.
- (4) A system has been established for selection of ball bearings for similar rotor support problems in vibration environment (assuming the Power Spectral Density is given).

FUTURE WORK

It was found that the criterion for brinelling damage in ball bearings is based on an arbitrary maximum Hertz stress level. This level has

been arrived at in bearing technology by static load tests on ball-race configurations. For applications where minimum bearing size is required a more accurate criterion should be established. We recommend that selected rolling contact bearings be subjected to vibration evaluations in which the maximum bearing load as determined from the analysis in this summary be varied over a range selected to cover nonbrinelling and brinelling levels. The extent of damage would then be evaluated on the basis of noise level during rotation under steady state load.

APPENDIX A

ANALYSIS OF FAN BEARING LOADS FROM RANDOM VIBRATION

APPENDIX A

ANALYSIS OF FAN BEARING LOADS FROM RANDOM VIBRATIONS

The dynamic response of the fan rotor assembly in the axial direction can be estimated by using the linear single-degree-of-freedom model shown in Figure A-1.

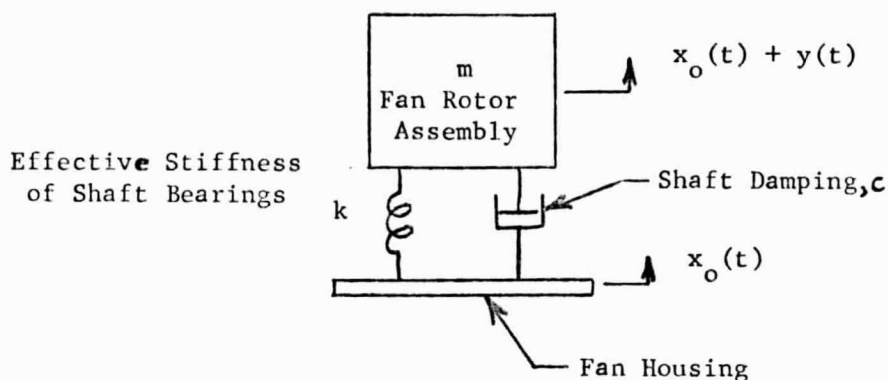


FIGURE A-1. SINGLE-DEGREE-OF-FREEDOM MODEL FOR DYNAMIC ANALYSIS

The axial motion of the rotor relative to its housing is of primary interest and the equation of motion is

$$m\ddot{y} + c\dot{y} + ky = -m\ddot{x}_o, \quad (\text{A-1})$$

which is often written in the form

$$\ddot{y} + \left(\frac{\omega_n}{Q}\right)\dot{y} + \omega_n^2 y = -\ddot{x}_o. \quad (\text{A-2})$$

where

$$\omega_n = (k/m)^{0.5} \text{ natural frequency} \quad (\text{A-3})$$

$$Q = m\omega_n / c \quad (\text{A-4})$$

y = axial displacement of the fan rotor relative to fan housing.

A-2

m = fan rotor assembly mass
 k = effective axial stiffness of the rotor bearing supports
 x_o = axial displacement of the fan housing.

The solution of Equation A-2 for random vibration can be expressed as (see Reference A-1 or other standard texts)

$$W_y(f) = |H(f)|^2 W_o(f), \quad (A-5)$$

$$|H(f)|^2 = \frac{1/(4\pi^2)^2}{(f_n^2 - f^2)^2 + (f_n^2 f^2)/Q^2}, \quad (A-6)$$

where

f = excitation frequency, Hz
 f_n = rotor natural frequency ($\omega_n/2\pi$), Hz
 $W_y(f)$ = displacement response, power spectral density
 $W_o(f)$ = acceleration excitation, power spectral density,

This gives the response as a function of frequency. In order to be useful, an estimate of the maximum expected displacement of the rotor relative to its housing is needed. This can be obtained by first calculating the root mean square (rms) of the displacement response from

$$y_{rms} = \sqrt{\overline{y^2}} = \left[\int_0^\infty W_y(f) df \right]^{1/2}, \quad (A-7)$$

and then making a statistical approximation that the maximum expected rotor displacement, y_{max} , will be no greater than three times the rms displacement.

$$y_{max} = e(y_{rms}). \quad (A-8)$$

Reference A-1. Crandall, S. H., and Mark, W. D., "Random Vibration in Mechanical Systems", Academic Press, 1963, pp 77-80

Therefore, the problem is reduced to evaluating the integral in Equation A-7 using the relations in Equations A-5 and A-6 and the power spectral density (PSD) of the vibration environment for the fan housing shown in Figure A-2. However, in order to avoid evaluating a complicated integral, the result is usually approximated by replacing the complex spectrum shown in Figure A-2 by a constant spectrum for white-noise with the amplitude determined by the amplitude of the real PSD at the natural frequency of rotor. The validity of this approximation is based on the knowledge that a low-damped single-degree-of-freedom system is highly responsive to excitation at frequencies very close to its natural frequency and relatively insensitive to excitation at frequencies much lower or higher than its natural frequency. Thus, the response can be predicted quite accurately by using a constant value of the excitation spectrum so long as this is an accurate level in the resonant bandwidth of the rotor. This resonant bandwidth depends on the damping and can be checked by

$$f_1 = f_n \left(1 - \frac{1}{2Q}\right), \quad (A-9)$$

$$f_2 = f_n \left(1 + \frac{1}{2Q}\right), \quad (A-10)$$

where f_1 and f_2 define the frequency bandwidth of interest centered at the rotor natural frequency f_n .

Using the approximation of replacing a complex PSD by a constant level white-noise spectrum with the excitation levels identical at the rotor natural frequency makes it possible to use a standard result from vibration texts (see Reference A-1). Equation A-7 then becomes

$$y_{\text{rms}} = \left[\frac{W_0 g^2 Q}{32 \pi^3 f_n^3} \right]^{\frac{1}{2}} \quad (A-11)$$

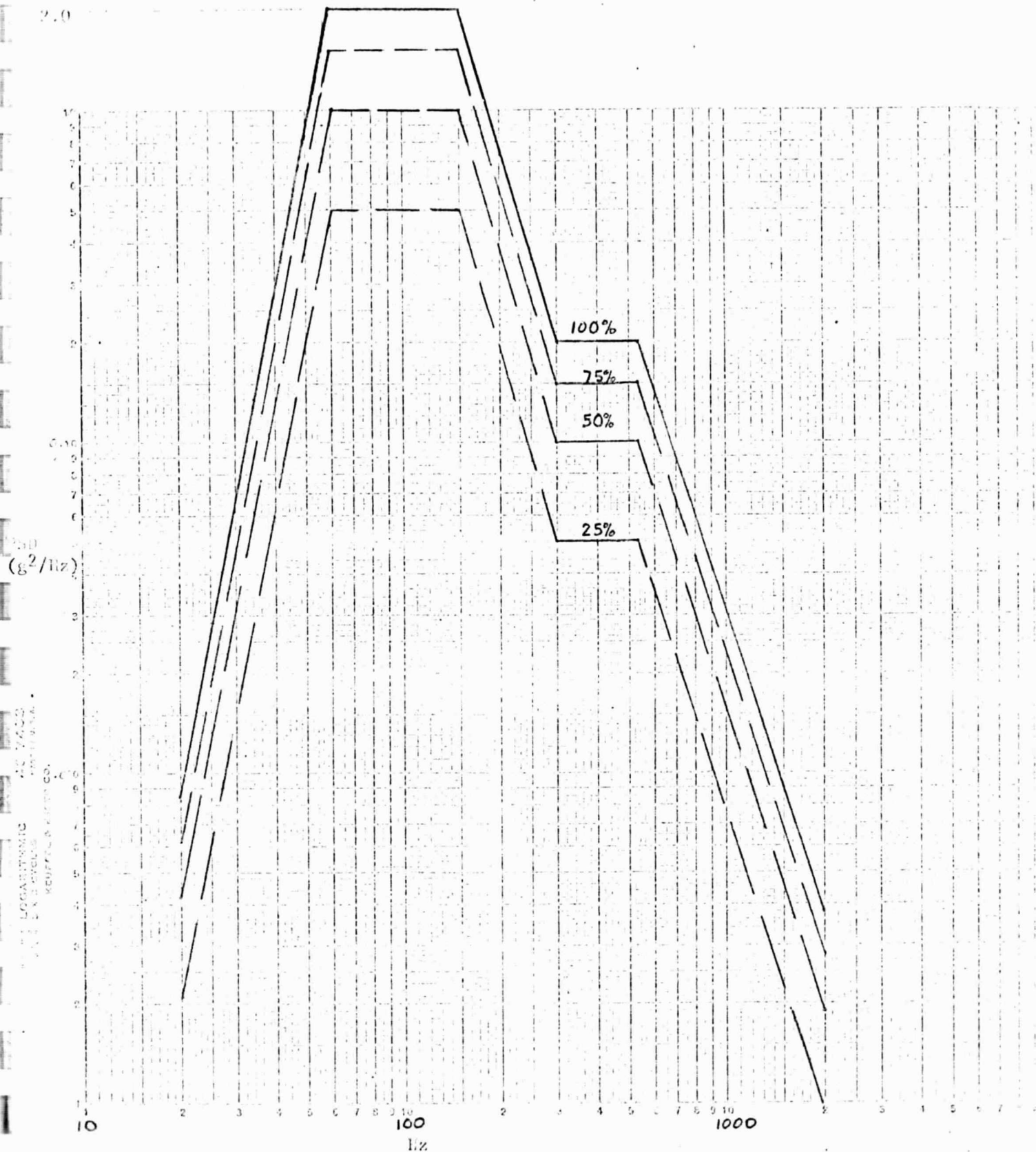


FIGURE A-2. POWER SPECTRAL DENSITY OF VIBRATION ENVIRONMENT FOR PLV FAN (REFERENCE MSFC MEMORANDUM S&E-ASTN-EME-69-243)

$$y_{\text{rms}} = 12.26 \left[\frac{W_o Q}{f_n^3} \right]^{\frac{1}{2}} \quad (\text{A-12})$$

and

$$y_{\text{max}} = 36.78 \left[\frac{W_o}{f_n^3} \right]^{\frac{1}{2}} \quad (\text{A-13})$$

where

$W_o(f_n)$ = test PSD at rotor natural frequency, g^2/Hz

g = acceleration of gravity, (386 in./sec²)

f_n = rotor natural frequency, Hz

Q = rotor amplification factor.

The maximum force which will be transmitted between the housing and the rotor through the bearings F_b is given by

$$F_b = k \sqrt{1 + \frac{1}{Q^2}} (y_{\text{max}}), \quad (\text{A-14})$$

or

$$F_b = (2\pi)^2 m f_n^2 \sqrt{1 + \frac{1}{Q^2}} (y_{\text{max}}). \quad (\text{A-15})$$

Example Calculation

To illustrate the use of Equations A-13 and A-15 for estimating the maximum expected axial displacements of the rotor and the bearing forces, the following parameters for the original fan configuration using one or more wave washers have been selected.

$f_n = 494 \text{ Hz}$ (from experimental measurements)

$Q = 44$ (from experimental measurements)

$m = 1.2/386 = 0.00311 \text{ lb sec}^2/\text{in.}$

$$W_o = 0.2 \text{ g}^2 \text{ Hz (100\% level at 494 Hz from Figure A-2)}$$

$$k = (2\pi)^2 m f_n^2 = (2\pi)^2 (0.0031) (494)^2 = 29,962 \text{ lb/in.}$$

$$y_{\max} = 36.78 \left[\frac{W_o Q}{f_n^3} \right]^{\frac{1}{2}} = 36.78 \left[\frac{0.2(44)}{(494)^3} \right]^{\frac{1}{2}} = 0.0099 \text{ inch}$$

$$F_b = k \sqrt{1 + \frac{1}{Q^2}} (y_{\max}) = 29,962 \sqrt{1 + \frac{1}{44^2}} (0.0099) = 297 \text{ lb.}$$

Since this force would be transmitted through a single bearing, it substantially exceeds the predicted allowable bearing force of 43 pounds.

To check the validity of the "white-noise" approximation for this analysis, the frequency bandwidth for the rotor can be calculated using Equations (A-9) and (A-10).

$$f_1 = f_n \left(1 - \frac{1}{2Q}\right) = 494 \left(1 - \frac{1}{88}\right) = 488 \text{ Hz,}$$

$$f_2 = f_n \left(1 + \frac{1}{2Q}\right) = 494 \left(1 + \frac{1}{88}\right) = 500 \text{ Hz.}$$

Because of the very low damping (high Q), the resonant bandwidth is very narrow and the "white-noise" approximation should be entirely adequate. The principle source of difference between analytical predictions of maximum bearing forces and the actual bearing forces which will occur during tests will be the nonlinearities of the bearings and preload spring. Measurements show that when the bearings are preloaded with any type of soft spring at one end of the shaft, the rotor natural frequency will be reduced and the damping will increase (lower Q) as the excitation amplitude is increased.

APPENDIX B

ANALYSIS OF THE ANGULAR CONTACT BALL BEARING
FOR AXIAL THRUST LOAD

APPENDIX B

ANALYSIS OF THE ANGULAR CONTACT BALL BEARING FOR AXIAL THRUST LOAD

This analysis was essentially derived from the book by Harris. Equations (2.6) through (2.10) and (2.25), (2.26), (5.30), (5.42), (6.26), (6.33), and (9.32) through (9.35) yield all the necessary information to perform this analysis. The appended computer code AXLOD utilizes these relationships. The program requires the inner race diameter (DI) (inches) ball diameter) (D) (inches) diametral clearance (PD) (inches) total curvature of the bearing ($B=f_i+f_o-1$), number of balls in the bearing (NB), increment in the contact angle (DLF) (radians) at which load, deflection and other parameters are sought, and the limit of the maximum Hertz pressure (PLM) (psi) beyond which the program should be terminated, as input parameters. The output consists of thrust load (lbs) and axial displacement (in.), the Hertz stress (psi), the corresponding minimum angle (radians) and land height (in.) required at the inner and outer race. These output quantities are calculated at intervals determined by the parameter (DLF). For $PD = 0.00065$ (in.) and $B=0.14$ the load-deflection calculated by this program agree with the corresponding quantities provided by Barden Corp. for the PLV fan bearings. In the method developed by Harris the analysis of angular contact ball bearings is dependent upon a certain constant derived by Jones which is usually read from a plot. In the computer code described here, Jones' assumptions about his constant are accepted but the value of the constant is computed within the program. It is assumed that the bearings consist of steel with Young's modulus of 30×10^6 psi and Poissons ration of 0.3.

PROGRAM AXLOD

AXLOD 15:46 CY FRI 04/24/70

```
100 DIMENSION SMCR(2), FRO(2), CDEL(2), FHRZ(2), ASTR(2)
110 COMMON FR,XE,XK
120 EXTERNAL FUNC1
130 PI = 3.1415926536
140 INPUT, DI, D, PD, B, NB, DLF, PLM
150 PRINT, " INN. RACE DIA., BALL DIA., DIA. CLEARANCE, B, NO. OF
160 + BALLS AND INCREMENT IN ALFA, MAX HERTZ LIMIT "
170 PRINT, DI, D, PD, B, NB, DLF, PLM
180 A = B*D ; ALO=ACOS(1.-PD/2./A) ; ENDP=2.*A*SIN(ALO)
190 CMP=(B+1.)/2. ; RCRD=CMPI*D
200 SMCR(1)=4./D+2./DI-1./RCRD
210 FRO(1)=(2./DI+1./RCRD)/SMCR(1)
220 RO=PD/2.+D+DI/2.
230 SMCR(2)=4./D-1./RO-1./RCRD
240 FRO(2) = (1./RCRD-1./RO)/SMCR(2)
250 BL=0.005 ; BU=0.9995 ; ERR=0.00001 ; N=20
260 DO 4 KOUNT = 1,2
270 FR = FRO(KOUNT)
280 EMD = YNEST(BL,BU,ERR,FUNCI,N,I,NTRY)
290 IF (I-0) 5,5,6
300 6 PRINT, " MODULUS, DID NOT CONVERGE,KOUNT,I,NTRY",KOUNT,I,NTRY
310 5 CONTINUE
320 AKAP = 1./EMD
330 ASTR(KOUNT)=(2.*AKAP*AKAP*XE/PI)**(1./3.)
340 BSTR = (2.*XE/AKAP/PI)**(1./3.)
350 CDEL(KOUNT)=(SMCR(KOUNT)*EMD*EMD*D/XE)**(1./3.)*XK
360 FHRZ(KOUNT)=(D*SMCR(KOUNT))**(2./3.)*100000./4.327/BSTR
362 + /ASTR(KOUNT)
370 4 CONTINUE
380 SM = CDEL(1)+CDEL(2)
390 ABJ = (B*1.E+06/SM/7.4858795)**1.5 ; ABJ3=ABJ**(1./3.)
400 PRINT, " SM,ABJ", SM,ABJ,+
410 PRINT, " THRUST LOAD, AXL. DSPL.",+
420 PRINT, " RACE, HERTZ PRESSURE, MIN, ANGLE AND LAND
425 + HEIGHT "
430 FTHR=NB*D*D*ABJ
440 AL = ALO
450 DO 10 J=1,100
460 AL = AL+DLF ; FCOS=SQRT(COS(ALO)/COS(AL)-1.)
470 THRST = FTHR*SIN(AL)*FCOS**3
480 DSPL = B*D*SIN(AL-ALO)/COS(AL)
485 PRINT, THRST, DSPL
490 DO 15 K = 1,2
500 FHRZ = FHRZ(K)*FCOS*ABJ3
510 THT = 0.009*ABJ3*ASTR(K)*FCOS/((D*SMCR(K))**(1./3.))
515 THT = ASIN(THT)+AL
520 HL = (1.-COS(THT))*D
530 IF(K-2) 16,17,17
540 16 PRINT 20, FHRZ, THT, HL
550 20 FORMAT(15X, " INNER", 3E15.4)
560 GO TO 14
570 17 PRINT 21, FHRZ, THT, HL
580 21 FORMAT(15X, " OUTER", 3E15.4)
590 14 IF(FHRZ-PLM) 15,25,25
600 IF ( THT-PI/2.) 15,25,25
610 15 CONTINUE
620 10 CONTINUE
630 25 STOP ; END
640 $USE PART2
```

OLD FILE NAME--PART2

READY.

LISTNH

```
1000 FUNCTION FUNC1(Z)
1010 COMMON FRO,XE,XK
1020 ZZ = SQRT ( 1.-Z*Z )
1030 AKAP = 1./Z ; XE = ELE(ZZ) ; XK = ELK(ZZ)
1040 FUNC1 = FRO-((AKAP*AKAP+1.)*XE-2.*XK)/XE/(AKAP*AKAP-1.)
1050 RETURN ; END
1060 FUNCTION ASIN(X)
1070 ASIN = ATAN(X/SQRT(1.-X*X))
1080 RETURN ; END
1110 FUNCTION ACOS(X)
1120 ACOS = ATAN(SQRT(1.-X*X)/X)
1130 RETURN ; END
1140 FUNCTION YNEST(BL,BU,E,FUNC,N,I,NTRY)
1150 DIMENSION A(3),B(3)
1160 NTRY=0
1170 NZ=0
1180 B(1)=BL
1190 B(3)=BU
1200 I=0
1210 35 A(1)=FUNC(B(1))
1220 IF(ABSF(A(1))-E)333,333,334
1230 333 YNEST=B(1)
1240 RETURN
1250 334 A(3)=FUNC(B(3))
1260 IF(ABSF(A(3))-E)335,335,336
1270 335 YNEST=B(3)
1280 RETURN
1290 336 P=A(1)*A(3)
1300 IF(P)25,24,24
1310 24 YNEST=0.
1320 I=2
1330 PRINT 1,B(1),A(1),B(3),A(3)
1340 1 FORMAT (" ROOT NOT NESTED, BL=",E15.8,5X,"L FUNC=",E15.8/
1350 +5X,"BU=",E15.8,5X,"U FUNC=",E15.8)
1360 RETURN
1370 25 DO 5 J=1,N
1380 NTRY=J
1390 B(2)=(B(1)+B(3))/2.
1400 A(2)=FUNC(B(2))
1410 IF(ABSF(A(2))-E)26,26,27
1420 26 YNEST=B(2)
1430 RETURN
1440 27 BP=RTF(B,A)
1450 AP=FUNC(BP)
1460 IF(ABSF(AP)-E)9,9,10
1470 10 P=A(2)*A(3)
1480 IF(P)11,12,12
1490 12 A(3)=A(2)
1500 B(3)=B(2)
1510 GO TO 13
1520 11 A(1)=A(2)
```

```

1530      B(1)=B(2)
1540 13 P=AP*A(3)
1550      IF(P)15,15,16
1560 16 A(3)=AP
1570      B(3)=BP
1580      GO TO 5
1590 15 A(1)= AP
1600      B(1)= BP
1610      5 CONTINUE
1620      I=1
1630      9 YNEST=BP
1640      RETURN
1650      END
1660      FUNCTION RTF(X,Y)
1670      DIMENSION X(3),Y(3)
1680      A=(Y(3)+Y(1)-2.*Y(2))/2.
1690      B=(Y(3)-Y(1))/2.
1700      C=Y(2)
1710      CHK=(ABSF(B)+ABSF(C))*1.E-4
1720      IF(ABSF(A)-CHK)20
1730      D=SQRTF(B*B-4.*A*C)
1740      XM=(-B-D)/2./A
1750      IF(ABSF(XM)-1.)21,21,25
1760 25 XM=(-B+D)/2./A
1770      GO TO 21
1780 20 XM=- (C/B+A*C/B/B/B)
1790 21 RTF=X(2)+(X(3)-X(2))*XM
1800      RETURN
1810      END
1820      FUNCTION ELK(X)
1830      IF(X*X-.5)10,10,20
1840 10 S=1.
1850      Q=1.
1860      DO 3 N=1,100
1870      U=N
1880      Q=Q*(U-.5)*X/U
1890      D=Q*Q
1900      S=S+D
1910      IF(ABS(D)-1.E-13)2,3,3
1920      3 CONTINUE
1930      PRINT 5
1940      5 FORMAT (1X,3HDI V)
1950      2 ELK=S*3.14159265358979/2.
1960      RETURN
1970 20 Y1=1.-X*X
1980      Y=SQRT(Y1)
1990      V=1.
2000      B=0.
2010      S=ALOG(4./Y)
2020      DO 6 M=1,100
2030      U=M
2040      V=V*(.5-U)/U*Y
2050      B=B+1./U/(2.*U-1.)
2060      D=V*V*(ALOG(4./Y)-B)
2070      S=S+D
2080      IF(ABS(D/S)-1.E-13)7,6,6
2090      6 CONTINUE
2100      PRINT 5
2110      7 ELK=S
2120      RETURN
2130      END

```

```

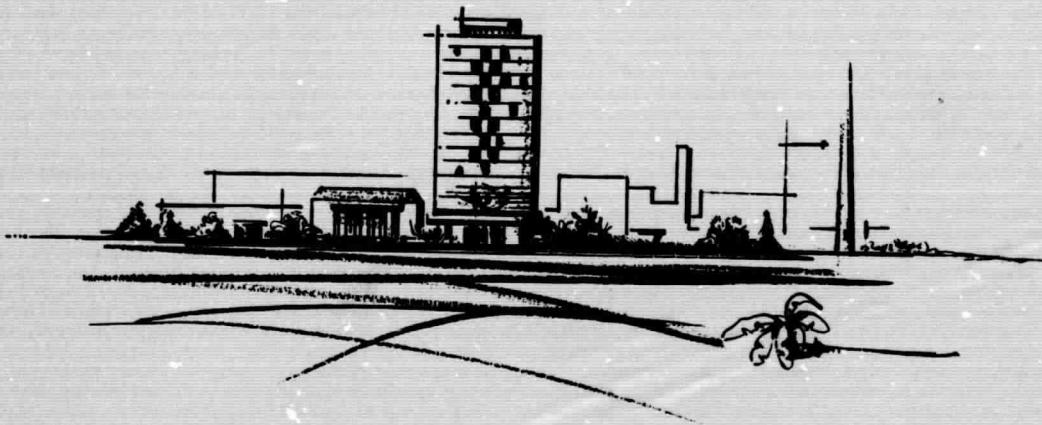
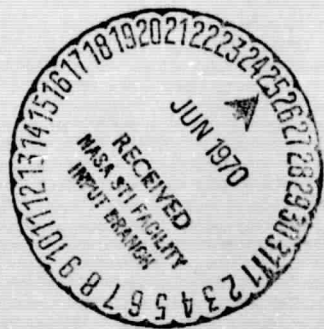
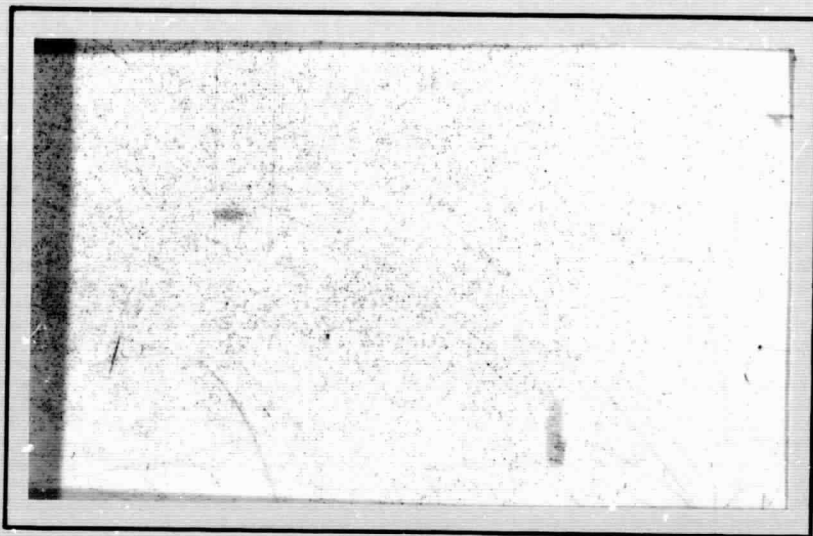
2140      FUNCTION ELE(X)
2150      IF(X*X-.5) 10, 10, 20
2160 10 S=1.
2170      V=1.
2180      DO 2 N=1, 100
2190      U=N
2200      V=V*(.5-U)/U*X
2210      D=V*V/(1.-2.*U)
2220      S=S+D
2230      IF(ABS(D)-1.E-13) 3, 2, 2
2240      2 CONTINUE
2250      PRINT 5
2260      5 FORMAT(1X, 3H DIV)
2270      3 ELE=S*3.14159265358979/2.
2280      RETURN
2290 20 Y1=1.-X*X
2300      IF(Y1) 22, 22, 21
2310 22 ELE=1.
2320      RETURN
2330 21 Y=SQRT(Y1)
2340      S=1.+(2.*ALOG(4./Y)-1.)*Y*Y/4.
2350      V=Y/2.
2360      C=1.
2370      DO 6 M=1, 100
2380      U=M
2390      V=V*(U-.5)/U*Y
2400      C=C+1./U/(2.*U-1.)+1./(U+1.)/(2.*U+1.)
2410      D=V*V*(2.*U+1.)/(U+1.)*(2.*ALOG(4./Y)-C)
2420      S=S+D
2430      IF(ABS(D)-1.E-13) 7, 6, 6
2440      6 CONTINUE
2450      PRINT 5
2460      7 ELE=S
2470      RETURN
2480      END

```


no contact

get DRA

RESEARCH REPORT



BATTELLE MEMORIAL INSTITUTE

COLUMBUS LABORATORIES

FACILITY FORM 602

N71	22527	(THRU)
(ACCESSION NUMBER)	31	63
(PAGES)	1R-117855	(CODE)
(NASA CR OR TMX OR AD NUMBER)	15	(CATEGORY)

SUMMARY REPORT

on

ANALYSIS OF BRINELLING FAILURE OF BEARINGS
FROM VIBRATION TESTED PLV FANS

to

NATIONAL AERONAUTICS AND SPACE ADMINISTRATION
GEORGE C. MARSHALL SPACE FLIGHT CENTER

by

W. A. Glaeser, S. K. Batra, and R. H. Prause

June 8, 1970

BATTELLE MEMORIAL INSTITUTE
Columbus Laboratories
505 King Avenue
Columbus, Ohio 43201

TABLE OF CONTENTS

	<u>Page</u>
SUMMARY	1
STATEMENT OF THE PROBLEM	2
THE MODE OF ANALYSIS	2
Analysis of Failed Bearings	2
VIBRATION ANALYSIS	8
Dynamic Analysis Model	9
Experimental Measurements	14
Methods for Modifying Bearing Load Levels	16
Angular Contact Bearing Design Analysis	17
RECOMMENDED PROCEDURE FOR CHOICE OF BEARINGS IN SIMILAR FUTURE APPLICATIONS	31
CONCLUSIONS AND RECOMMENDATIONS FOR FUTURE WORK	33
FUTURE WORK.	33
APPENDIX A	
ANALYSIS OF FAN BEARING LOADS FROM RANDOM VIBRATIONS	A-1
Example Calculation	A-5
APPENDIX B	
ANALYSIS OF THE ANGULAR CONTACT BALL BEARING FOR AXIAL THRUST LOAD	B-1
PROGRAM AXLOD	

SUMMARY REPORT

on

ANALYSIS OF BRINELLING FAILURE OF BEARINGS
FROM VIBRATION TESTED PLV FANS

to

NATIONAL AERONAUTICS AND SPACE ADMINISTRATION

from

BATTELLE MEMORIAL INSTITUTE
Columbus Laboratories

SUMMARY

Brinelling damage has been identified in PLV fan bearings as the cause for noisy running after exposure to a random-vibration environment.

Assuming a maximum Hertz stress of 460,000 psi to produce brinelling, the maximum axial load for the fan bearing was calculated as 43 pounds. Dynamic analysis of the rotor-bearing-spring system revealed that with one preload spring, the maximum predicted axial load would be 297 pounds. Reduction in maximum bearing loads under vibration conditions can be achieved by reducing the rotor natural frequency and by increasing the damping through using a soft spring system. This means multiple springs at both ends of the shaft. When a system of five springs at each end of the rotor was considered, the bearing load predicted was 58 pounds. Actual vibration tests at Marshall Space Flight Center using the 5-spring preload configuration have resulted in reduction of bearing damage. Use of Belleville springs for this particular rotor-bearing configuration was found undesirable because the collapse load of the springs would be easily exceeded during the anticipated operating conditions.

A bearing load-capacity computer program was written so that, given the bearing parameters, inner race diameter, ball diameter, diametral clearance, total curvature of the race groove and number of balls, the limiting axial load can be determined using maximum Hertz stress and over-riding of the race land as the failure criteria.

STATEMENT OF THE PROBLEM

PLV fans subjected to acceptance vibration tests have developed rough running, noisy bearings. Brinelling of the bearing races was suspected as the cause of rough running. If brinelling has been the cause, then overloading of the bearings from inertial loads has occurred and can only be alleviated by increasing the size of the bearing or reducing the peak inertial loads. If fretting or "false brinelling" has been the cause of rough races, then load capacity of the bearing will have no significance in the severity of the effect. Brinelling is a plastic deformation process; fretting is a time-dependent wear process and the latter is a function of rubbing amplitude and lubrication.

THE MODE OF ANALYSIS

An analysis was performed on the rotor-bearing system to determine the following:

- (1) The nature of damage to fan bearings (whether it is brinelling or fretting).
- (2) The maximum bearing loads resulting from test random vibration environment.
- (3) Hertz stresses developed in the bearings and displacement of balls in races using the load values obtained in Number (2).
- (4) The influence of bearing preload and preload spring configuration on bearing contact stress levels.

Analysis of Failed Bearings

Samples of both new bearings and bearings from noisy fans were analyzed in the Battelle Lubrication Mechanics Laboratory. Bearings were disassembled and the race surfaces examined by stereoptican microscope. The race surface topography was measured with a Talyrond roundness instrument.

Microscopy revealed classic brinelling on the inner and outer races of bearings taken from tested fans. The following bearings were examined:

- (1) Used bearing with much of the grease gone. Severe brinelling over-running the lip of the ball groove.
brinelling on one side of the race groove.

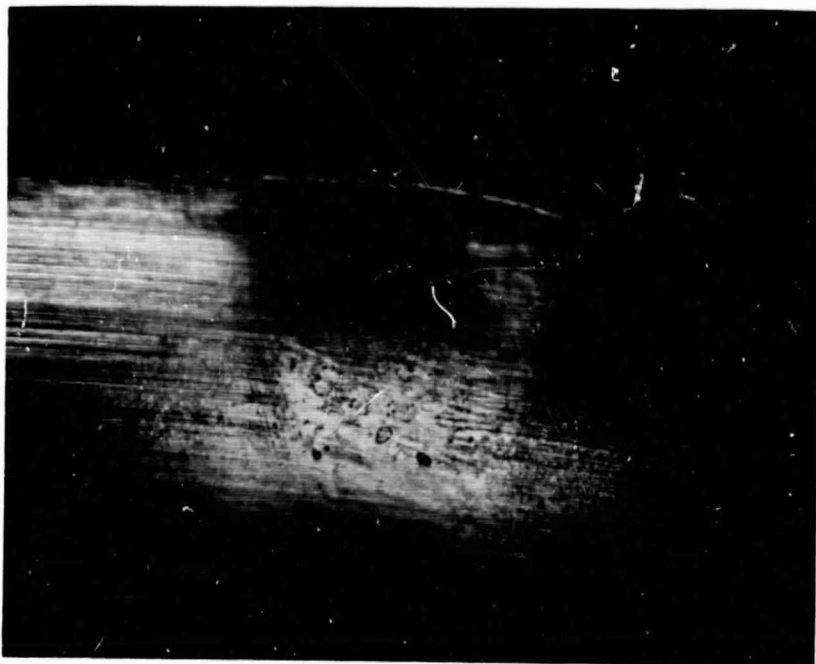
- (2) New bearing filled with grease. All surfaces free of defects.
- (3) Used bearing with much of the grease gone. Mild brinelling on inner and outer races.
- (4) Used bearing with some residual grease. One set of brinell marks on inner race and barely visible on outer race.
- (5) Used bearing full of grease. Very light brinell marks on inner and outer races.

The extent of ball indentation in the severely brinelled bearing is shown in the photomicrograph in Figure 1.

Talyrond measurements were made on several circumferential positions of the inner races of the bearings. The traces were made with the stylus riding (1) on the bottom of the ball groove, (2) on the side of the ball groove, and (3) on the race lands. Typical traces of brinelled bearings are shown in Figures 2, 3, and 4. The location of the tracing stylus is shown in the drawing at the top of each tracing. For instance, the trace in Figure 2a was made on the race land.

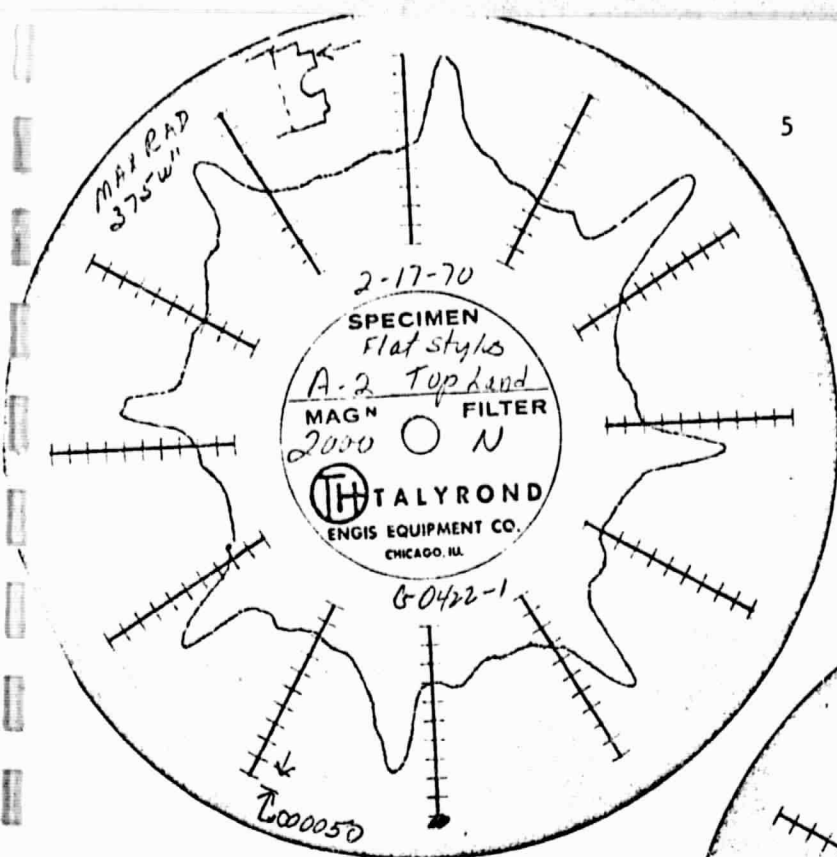
Figure 2 shows an example of heavy brinelling. The bearing was so overloaded axially that the balls were driven up the sides of the ball groove and indented the lip causing a mounding up on the race land surface. The mounding up can be seen in Figure 2a. Each mound represents the position of one ball in the bearing. All eight balls have produced indentations. The height of the mounds averaged 0.00025 inch. The indentations in the thrust side of the ball groove can be seen in Figure 3. The trace indicates one set of severe brinell marks together with at least two other sets of lighter brinell marks. Apparently this bearing was subjected to several separate conditions of axial vibration, one of them being most severe. Average depth of the severe indentations was about 0.00025 inch. Width of the indentations at the surface averaged about 0.03 inch. (The proportions of the indentations are distorted on the Talyrond traces because radial magnification is much higher than circumferential.)

The brinell marks did not extend into the bottom of the race groove as shown in the trace in Figure 2b. The trace is smooth, and slightly egg-shaped,

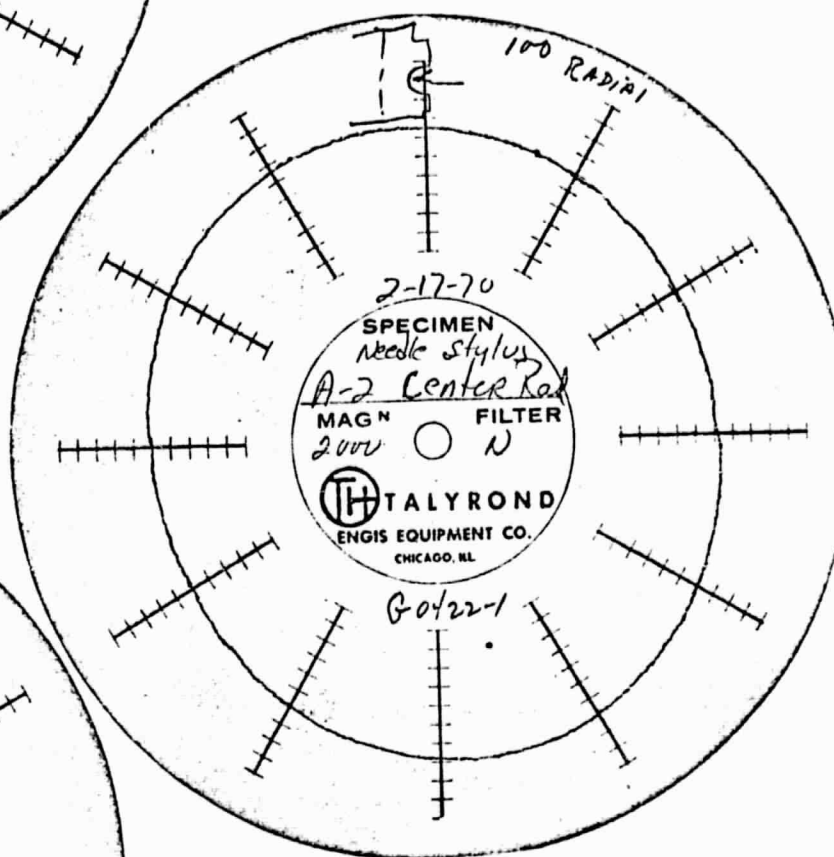


75 X

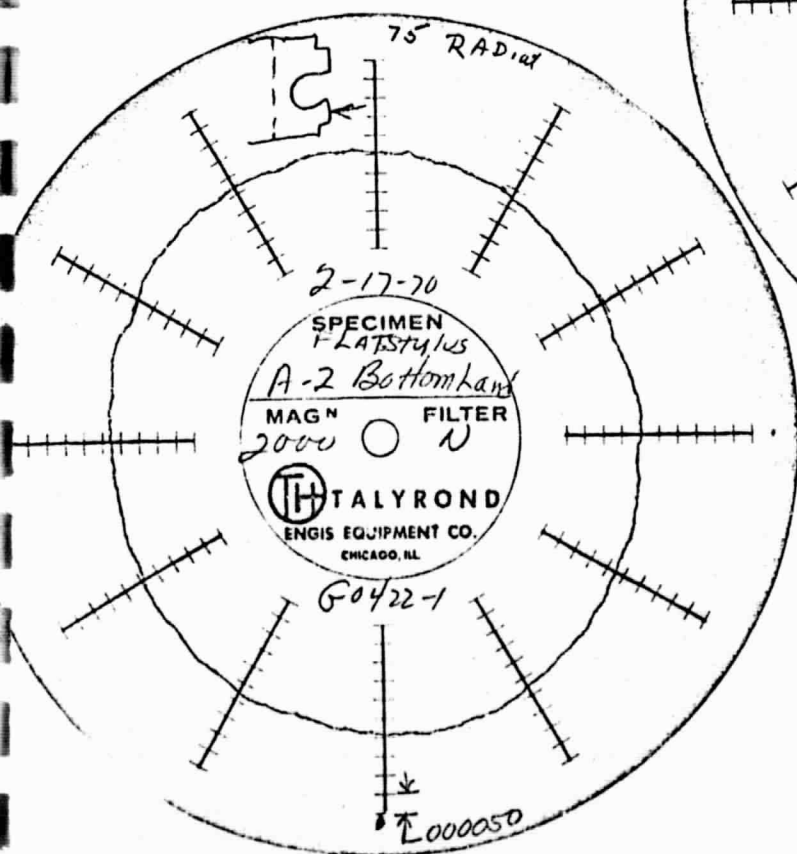
FIGURE 1. SEVERE BRINELLING DAMAGE ON INNER RACE OF FAN BEARING. THE PHOTOGRAPH SHOWS ONE BALL INDENTATION EXTENDING OVER THE RACE GROOVE LIP



a. Land surface



b. Bottom of race groove



c. Land surface

FIGURE 2. TALYROND TRACES OF SEVERELY BRINELLED
FAN BEARING INNER RACE

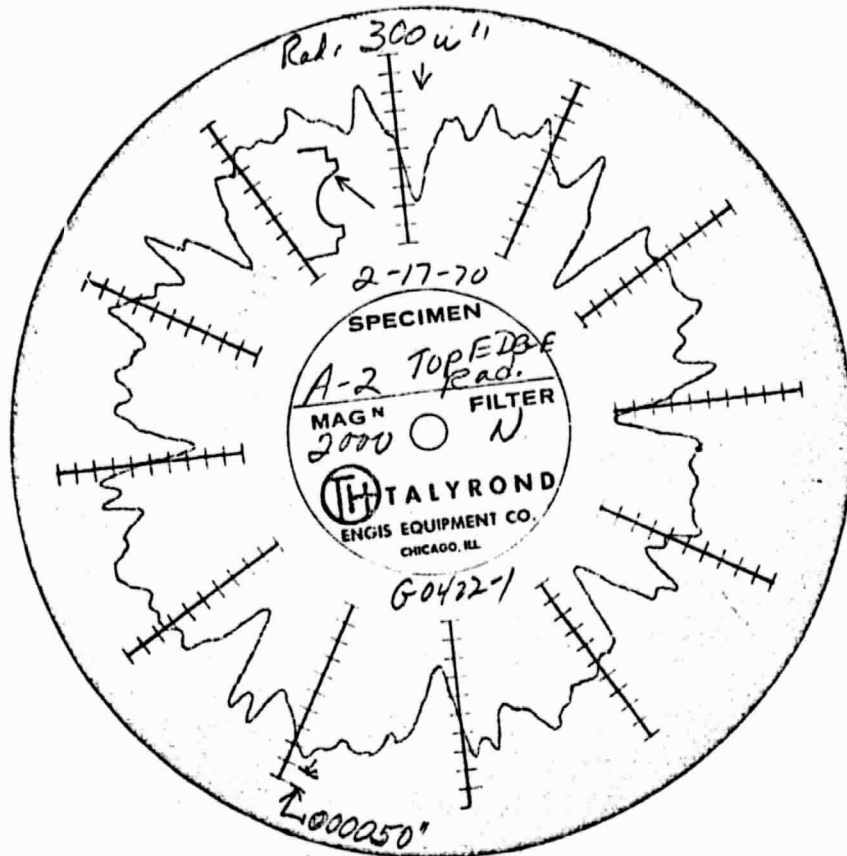
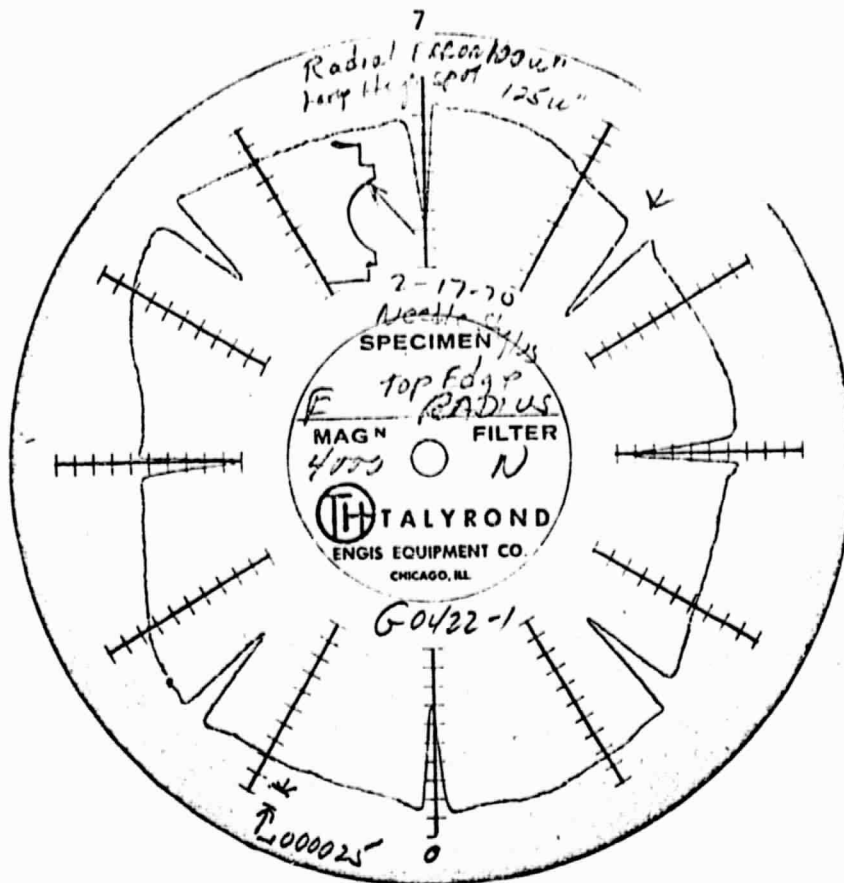
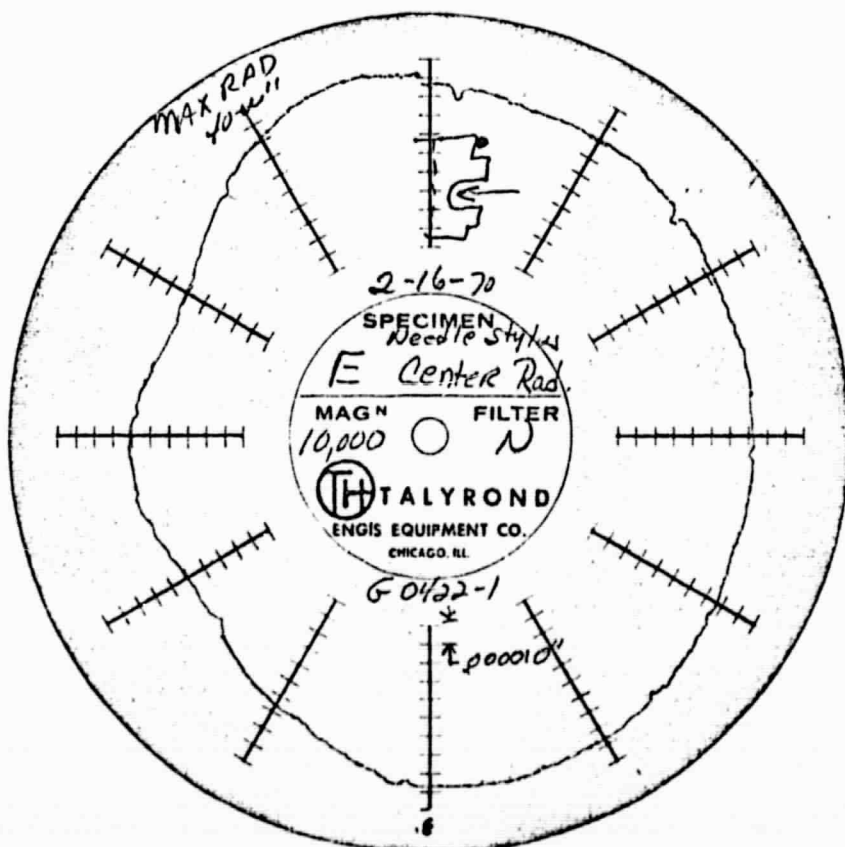


FIGURE 3. TALYROND TRACE OF SEVERELY BRINELLED FAN BEARING INNER RACE TAKEN ON THE THRUST SIDE OF THE RACE GROOVE



a. Thrust side of race groove



b. Bottom of race groove

FIGURE 4. TALYROND TRACES OF LIGHTLY BRINELLED FAN BEARING INNER RACE

indicating ovality in the race geometry. It was concluded, therefore, that brinelling damage was associated with axial loads and not radial loads.

An example of light brinelling damage is shown in Figure 4. These marks were barely visible under the microscope. Maximum depth of the indentations are about 0.0001 inch. Note that faint indications of light dents show up in the trace made of the bottom of the ball groove. This indicates that the balls were not displaced as far from their no-load position as they were in the bearing exhibiting heavy brinelling. In addition, the trace shows only one set of brinell marks in this bearing. If the bearing was subjected to more than one vibration condition only one was severe enough to produce damage.

It has been concluded from the examination of failed bearings that the damage is true brinelling resulting from inertial overloads and that the conformity and radial play conditions in these bearings allow sufficient relative motion of rolling elements under axial load so that ball over-riding of the race groove lip is possible under heavy enough load.

VIBRATION ANALYSIS

An important objective of this program was to establish an analytical method for estimating maximum bearing loads when the PLV fan was subjected to a random vibration environment. Calculated bearing loads could then be used to compare the predicted results with the experience from tests where bearings have failed, and to evaluate proposed modifications to the bearing support system in order to select a modification most promising for further testing.

Equations for predicting the maximum expected rotor displacements and bearing loads have been derived and a detailed development is included in Appendix A, with numerical examples to demonstrate correct application. These equations are based on certain simplifying assumptions regarding the shape of the power spectrum of the vibration test specifications, as well as the use of a linear spring representation for the shaft bearings and preload springs, which are actually quite nonlinear. Even so, it is believed that this idealized model is a useful design tool.

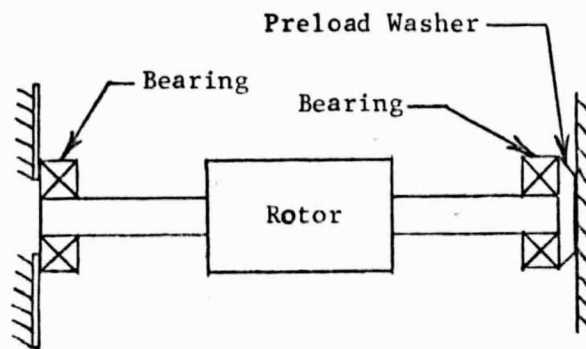
Dynamic Analysis Model

Figure 5a is a sketch of the original configuration of the fan rotor and bearings¹ using one wave washer to obtain a 6 pounds axial preload. Figure 5b shows springs representing the flexibility of the bearings and preload washer, and this is transformed to the equivalent single-degree-of-freedom model shown in Figure 5c. The washer is very flexible relative to the bearings. Therefore, the only contribution of the washer is to establish sufficient preload so that for small motions about the shaft equilibrium position, the total effective stiffness is that of the one bearing that is preloaded against the rigid housing.

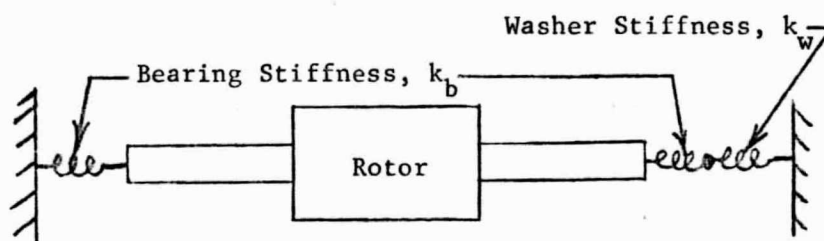
When the shaft deflection exceeds the 0.005 inch preload deflection, the bearing will be unloaded, and the effective stiffness will be that of the wave washer. Figure 6 shows the load-deflection curves for several different preloads to demonstrate how the bearing stiffness is the important parameter in determining the effective axial stiffness. These curves also show the net external force limitations imposed by the 43 pounds maximum axial load capability of the bearings. There will be no significant change in these curves if multiple washers are used to replace the single washer so long as they are all on one end of the shaft and the total preload force is the same.

If, however, washers are installed at both ends of the shaft, Figure 7 shows that the stiffness of the flexible washers will be the determining factor of the total effective stiffness. Figure 8 shows several load-deflection curves for five Belleville springs stacked in parallel at each end of the shaft. The load-deflection characteristics obtained from MSFC Drawing SK20-5072 indicate these springs have a maximum load capability of about 14.5 pounds and Figure 8 shows this collapse load.

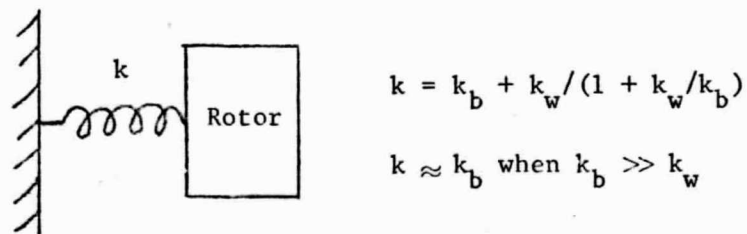
¹ The bearing considered in the analysis was Barden SR4SS, One-quarter-inch bore, angular contact, currently in use. Assuming a limiting maximum Hertz stress of 460,000 psi, the maximum axial load capacity of the bearing was determined as 43 pounds using the computer program described in the next section.



a. Bearing Support Configuration



b. Spring Model of Bearing Supports



c. Simplified Model for Dynamic Analysis

FIGURE 5. DEVELOPMENT OF MODEL REPRESENTING THE AXIAL DYNAMICS OF THE PLV FAN ROTOR ASSEMBLY WHEN PRELOADED BY FLEXIBLE WASHERS AT ONE END

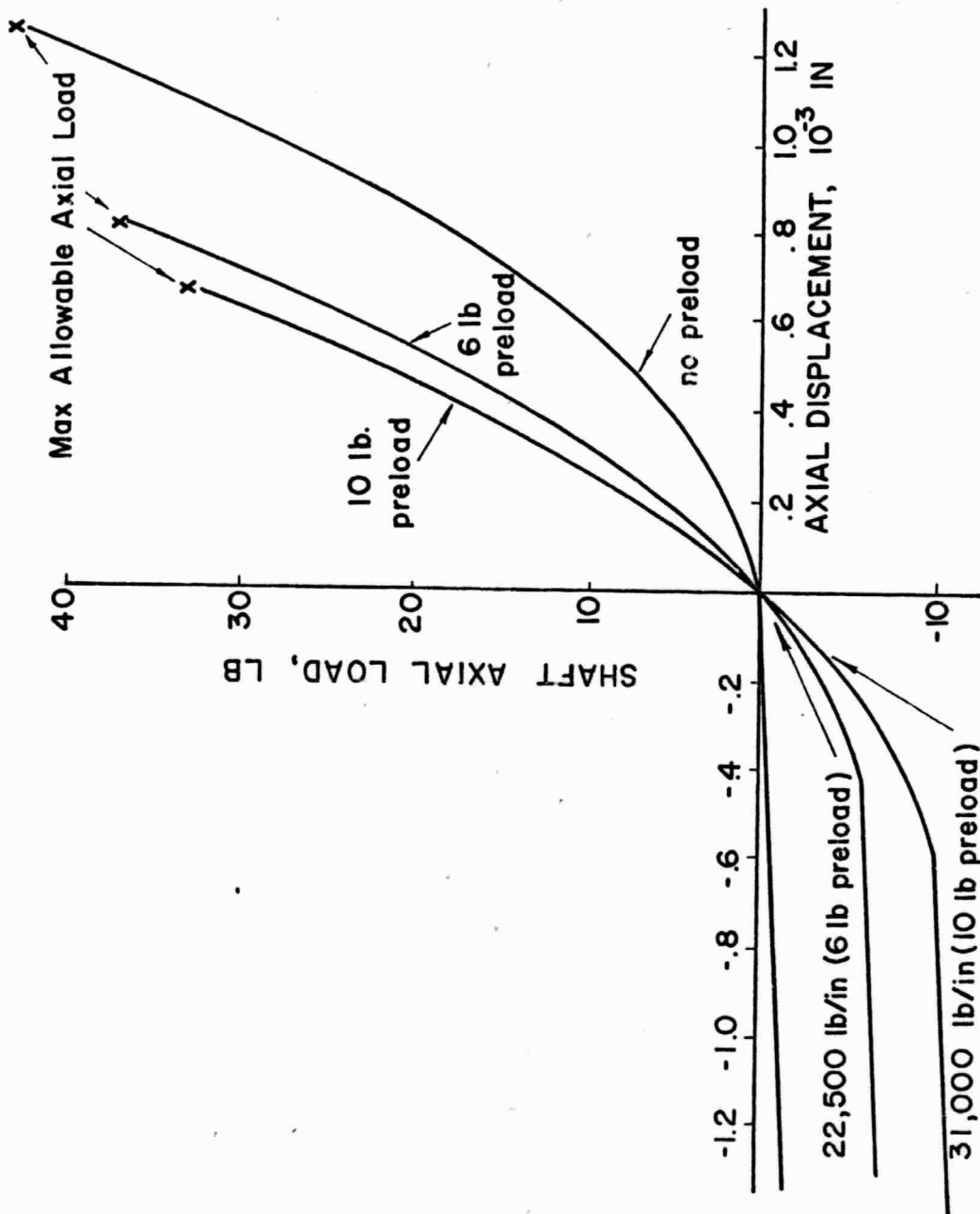
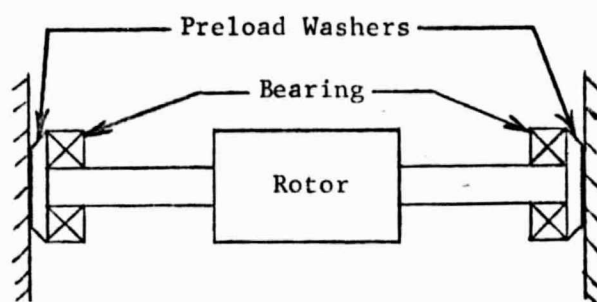
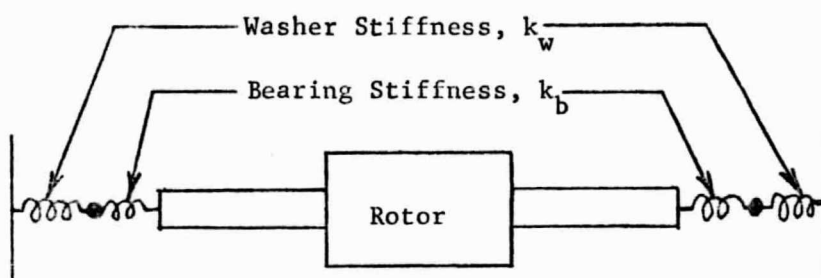


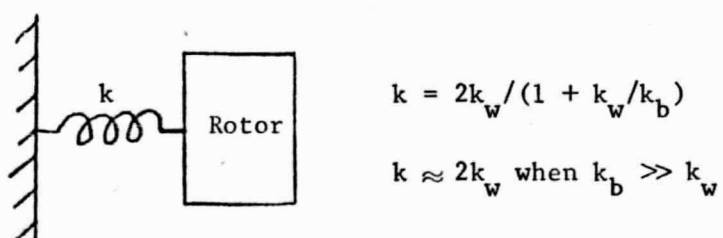
FIGURE 6. AXIAL LOAD-DEFLECTION CURVES FOR FAN SHAFT PRELOADED BY ONE WAVE WASHER AT ONE END



a. Bearing Support Configuration



b. Spring Model of Bearing Supports



c. Simplified Model for Dynamic Analysis

FIGURE 7. DEVELOPMENT OF MODEL REPRESENTING THE AXIAL DYNAMICS OF THE PLV FAN ROTOR ASSEMBLY WHEN PRELOADED BY FLEXIBLE WASHERS AT BOTH ENDS

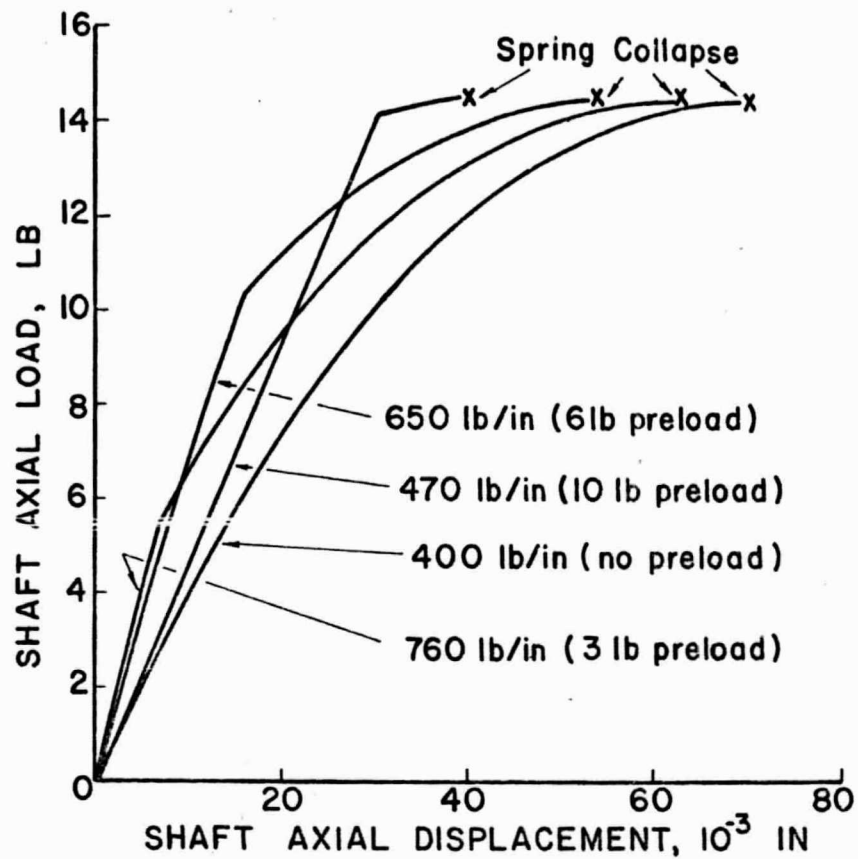


FIGURE 8. AXIAL LOAD-DEFLECTION CURVES FOR FAN SHAFT WITH FIVE BELLEVILLE SPRINGS AT EACH END STACKED IN PARALLEL

Experimental Measurements

In order to predict the maximum expected bearing loads using the equations derived in Appendix A, it is necessary to know the natural frequency and the resonant amplification factor Q of the rotor in the axial direction. The natural frequency can be predicted analytically, at least within the linear system approximations, but the Q of the system must be measured.

In order to measure both the natural frequency and effective damping (Q), the fan housing was clamped rigidly in a heavy vise and a soft rubber mallet was used to tap the rotor and produce a transient vibration. A Kistler Model 802-A piezoelectric accelerometer mounted on the fan impeller was used with a Kistler Model 568 charge amplifier, and the vibration signal was displayed on a Tektronix Type 502 oscilloscope. A Polaroid camera was used to record the transient vibration and the photographs were analyzed to determine the natural frequency and damping.

Table 1 summarizes the measured frequencies and Q factors for three bearing support configurations. Equations A-13 and A-15 in Appendix A were used to calculate the maximum expected bearing loads and rotor displacements. Although the calculated values of bearing loads for the original fan configuration (Configuration I) are probably higher than would be actually measured because of the neglected nonlinearities, it is evident that the bearing loads from the vibration tests are considerably higher than the 43 pounds maximum allowable load. The observed reduction in natural frequency at higher vibration amplitudes was caused by the rotor motion exceeding the washer preload so that the bearings were unloaded for part of each vibration cycle. The photographs of the transient vibration indicated that the preload was exceeded at an amplitude of about 0.004 inches (± 16 g's), which agrees closely with the design specifications for the wave washer.

With one Belleville spring installed at each end of the shaft, the calculated and measured natural frequencies were in close agreement and the damping was increased considerably (lower Q). However, the vibration environment is most severe in the frequency range of 60 to 150 Hz (see Figure A-2) so the predicted bearing loads are excessive and the Belleville springs would collapse.

TABLE 1. SUMMARY OF MEASURED ROTOR DYNAMIC CHARACTERISTICS AND PREDICTED BEARING LOADS FOR 100 PERCENT LEVEL VIBRATION TEST SPECIFICATIONS

Configuration	Rotor Natural Frequency, Hz		Q	Maximum Predicted Bearing Load, lb (3)	Maximum Predicted Rotor Displacement, inch
	Theoretical	Measured			
I. One Wave Washer at one end 6 lb design preload	427(4)	494(+10 g's) 440(+20 g's) 385(+80 g's)	44 24	297(1) 205(1)	0.0099 0.0087
II. One Belleville Spring each end Approximately 10 lb preload	138	125	11	118(1,2)	0.123
III. Five Belleville Springs each end Approximately 6 lb preload	73	100	3	58(1,2)	0.090

- (1) Exceeds maximum allowable bearing load.
 (2) Exceeds Belleville spring collapse load.
 (3) 100 percent Level Vibration Test Specification (MSFC Memo. S&E-ASTN-EME-69-243).
 (4) A 10 lb preload gives a 500 Hz theoretical natural frequency.

With five Belleville springs at each end (Configuration 3) the damping was increased considerably. The predicted loads were reduced sufficiently to suggest that the bearings might be capable of surviving the vibration tests, but the Belleville springs would be expected to collapse. It does not appear practical to use Belleville springs with a 14.5 pounds collapse load with bearings which have a 43 pounds allowable load.

Methods for Modifying Bearing Load Levels

Figure A-2 shows that the most severe vibration excitation is in the 60-540 Hz frequency range with reduced levels extending to the 20 Hz low frequency limit and to the 2000 Hz high frequency limit. In order to reduce the fan bearing loads it is obvious from Figure A-2 that to have reduced excititing forces either the natural frequency should be reduced considerably from the 494 Hz resonance of the original design configuration, or the system should be stiffened to increase its natural frequency. One advantage of reducing the natural frequency by supporting the rotor with flexible springs is that this type of modification will increase the damping and reduce the resonant amplification factor Q . If the natural frequency is increased, the damping will be quite low (high Q) as indicated by the measurements, and it is quite difficult to introduce additional damping in a high frequency system.

If it is assumed that $Q = 5$ is reasonable for a softly-sprung bearing mount, the maximum allowable bearing load of 43 pounds can be used to calculate a reasonable frequency suitable for a design goal. Results of this calculation show that the rotor axial natural frequency must be reduced below 55 Hz for the predicted bearing loads to be less than the maximum allowable. For a safety factor of 2, the natural frequency should be below 43 Hz, and the springs must permit the maximum expected rotor displacement of ± 0.19 inch.

These large relative displacements present practical problems because the radial clearance between the bearing O.D. and the bearing housing should be kept small for satisfactory fan operation. However, the bearings must be quite free axially to obtain the Required low natural frequency and large displacements. Slight misalignment or excessive friction could bind the bearings so that while a "soft" support system appears theoretically satisfactory, extreme care in manufacturing and assembly would be required to obtain high reliability using the current blaring mount configuration.

The alternative solution of rigidly mounting the bearings to obtain a high natural frequency eliminates the requirement of providing the axial motion. However, it would probably be necessary to increase both the bearing size and number of bearings. For example, if the highest measured value of $Q = 44$ is assumed, the natural frequency must be greater than 2000 Hz if the load on a single bearing is reduced below 43 pounds. If a pair of larger preloaded bearings are used with the rating of each bearing doubled to 86 pounds and the bearing stiffness is increased proportionately (actually the bearing stiffness may increase by a greater factor than the load rating), then the rotor natural frequency would be doubled (≈ 1000 Hz). The total predicted bearing force would be 164 pounds or 82 pounds per bearing, which would be acceptable. The maximum rotor displacement would be only 0.0013 inch. The limitation with this solution is that the bearing housing structure must be rigid relative to the bearings, and it is difficult to design a bearing system that will actually have a resonance as high as 1000 Hz without a severe weight penalty.

After examining the alternatives of either a soft, low-frequency bearing system or a stiff, high-frequency system, it does not appear that the present PLV fan configuration can be easily modified in order to pass the vibration tests and operate reliably. It is recommended that if the fan design is revised, the bearings should be soft-mounted in the axial direction with the flexible element attached rigidly to the bearing outer case to eliminate any sliding elements. Damping should either be obtained with the flexible element, such as the hysteresis loss in an elastomer, or a damping device introducing friction could be attached independent of the bearing supports.

Angular Contact Bearing Design Analysis

Essential features of the angular contact bearing design are reasonably well understood. The mathematical analysis of the geometrical parameters influencing the load capacity of the bearing is well detailed in the books by Harris² and Jones³. In estimating the load capacity of the bearing in the axial and/or radial direction the hydrodynamic effects of lubrication

² Tedric A. Harris, "Rolling Bearing Analysis", 1966, John Wiley & Sons, Inc.

³ A. B. Jones, "Analysis of Stresses and Deflection", Volume 1 and 2, Copyright 1946, New Departure, Division of General Motors Corp.

are generally ignored; the design criteria are based on the Hertz theory of dry-static contact between the rolling elements.

The formulations pertaining to thrust load, applied to single row angular contact bearing, have been employed in the analysis of the PLV for bearings. The appropriate mathematical equations have been adopted from Harris's book. Using these expressions a computer code was written for the G.E. Time Sharing System (Mark I); this is included and explained in Appendix B. This program was written with the intent of providing a useful tool for analyzing the influence of various geometric parameters on the load-deflection curve of PLV fan bearing. For instance for the bearings currently in use, assuming 57 percent conformity and diametral clearance of 0.00065 inch the value of the axial deflections were computed (computer output I) for various static loads.⁴ The load deflection curve is plotted in Figure 9; this curve was used in the dynamic analysis of the previous section.

To illustrate the use of the computer program several additional runs (computer outputs II-V) were made in which ball race conformity and the diametral clearance (contact angle)⁵ were selectively varied. To understand the output of the program reference may be made to the illustration in Figure 10. Here α designates the contact angle and θ_o (θ_i for the inner race) is the minimum angle the outer race must subtend, as shown, in order to avoid the riding of the ball over the land. H_o (H_i for the inner race) designates the minimum land height the outer race must possess in order to prevent ball over riding. All this is true for a given thrust load. The program computes these quantities as well as the maximum Hertz stress for both the inner and

⁴ The critical dimensions used in the analysis for the SR4SS bearing are as follows:

inner race diameter, d_i = 0.3401 inch (See Figure 10)
 ball diameter, D = 0.0937 inch
 number of balls = 8
 diametral clearance = 0.00065 inch
 B , or $(f_i + f_o - 1)$ = 0.14
 where f_i = inner race conformity
 f_o = outer race conformity

⁵ Diametral clearance and contact angle are related in the following way:

$$\alpha = \cos^{-1} \left(\frac{P_d}{2A} \right) \quad \text{where } \alpha = \text{contact angle} \quad \begin{array}{l} A = B \times \text{ball diameter} \\ B = f_o + f_i - 1 \end{array}$$

where P_d = diametral clearance

where f_o = outer race groove radius/ ball diameter
 f_i = inner race groove radius/ ball diameter.

COMPUTER OUTPUT I

IN PART2

FLV. BEARING MAXIMUM LOAD CAPACITY

? 0.340075, 0.09375, 0.00065, 0.148, 0.00453, 460000.

INN. FACE DIA., BALL DIA., DIA. CLEARANCE, E, NO. OF BALLS AND INCREMENT
IN ALFA.3401 .0937 6.5000E-04 .14 8
.0046

SM, ABJ 2.862 523222.75

THRUST LOAD, AXL. DSPL.

	RACE	HERTZ	PRESSURE, MIN.	ANGLE	LAND HEIGHT
.2352	6.17033E-05				
	INNER	.9401E+05	.2632E+00	.3352E-02	
	OUTER	.7783E+05	.2664E+00	.3307E-02	
.3363	1.23533E-04				
	INNER	.1337E+06	.2910E+00	.3913E-02	
	OUTER	.1103E+06	.2874E+00	.3845E-02	
1.592	1.85506E-04				
	INNER	.1646E+06	.3079E+00	.4410E-02	
	OUTER	.1364E+06	.3043E+00	.4321E-02	
2.5335	2.47612E-04				
	INNER	.1911E+06	.3240E+00	.4873E-02	
	OUTER	.1583E+06	.3203E+00	.4769E-02	
3.6725	3.09857E-04				
	INNER	.2148E+06	.3339E+00	.5331E-02	
	OUTER	.1780E+06	.3347E+00	.5203E-02	
4.9951	3.72246E-04				
	INNER	.2366E+06	.3529E+00	.5777E-02	
	OUTER	.1960E+06	.3483E+00	.5631E-02	
6.51	4.34732E-04				
	INNER	.2569E+06	.3663E+00	.6219E-02	
	OUTER	.2129E+06	.3614E+00	.6055E-02	
8.2224	4.97466E-04				
	INNER	.2761E+06	.3792E+00	.6661E-02	
	OUTER	.2238E+06	.3739E+00	.6478E-02	
10.1333	5.60304E-04				
	INNER	.2944E+06	.3918E+00	.7103E-02	
	OUTER	.2439E+06	.3861E+00	.6901E-02	
12.2649	6.23297E-04				
	INNER	.3120E+06	.4040E+00	.7547E-02	
	OUTER	.2584E+06	.3930E+00	.7327E-02	
14.6098	6.86450E-04				
	INNER	.3239E+06	.4159E+00	.7994E-02	
	OUTER	.2725E+06	.4096E+00	.7755E-02	
17.131	7.49765E-04				
	INNER	.3453E+06	.4277E+00	.8444E-02	
	OUTER	.2860E+06	.4210E+00	.8187E-02	
19.9871	8.13246E-04				
	INNER	.3612E+06	.4392E+00	.8899E-02	
	OUTER	.2992E+06	.4323E+00	.8623E-02	

COMPUTER OUTPUT I (CONTINUED)

23.1371	8.76396E-04			
	INNER	.3767E+06	.4506E+00	.9358E-02
	OUTER	.3121E+06	.4433E+00	.9063E-02
26.3412	9.40718E-04			
	INNER	.3919E+06	.4619E+00	.9822E-02
	OUTER	.3247E+06	.4543E+00	.9508E-02
29.9161	.001			
	INNER	.4068E+06	.4730E+00	.1029E-01
	OUTER	.3370E+06	.4651E+00	.9958E-02
33.7227	.0011			
	INNER	.4214E+06	.4840E+00	.1077E-01
	OUTER	.3491E+06	.4758E+00	.1041E-01
37.1662	.0011			
	INNER	.4353E+06	.4949E+00	.1125E-01
	OUTER	.3610E+06	.4864E+00	.1087E-01
42.2113	.0012			
	INNER	.4500E+06	.5057E+00	.1173E-01
	OUTER	.3723E+06	.4969E+00	.1134E-01
47.0000	.0013			
	INNER	.4639E+06	.5164E+00	.1222E-01

COMPUTER OUTPUT III

INN. RACE DIA., BALL DIA., DIA. CLEARANCE, B, NO. OF BALLS AND INCREMENT I
N ALFA, MAX HERTZ LIMIT

.3401 .0937 1.00000E-04 .1178 8
.0046 460000.00

SM, ABJ 2.7668 428927.06

THRUST LOAD, AXL. DSPL.

RACE, HERTZ PRESSURE, MIN, ANGLE AND LAND HEIGHT

.0287	5.10551E-05			
	INNER	.5543E+05	.1263E+00	.7465E-03
	OUTER	.4583E+05	.1252E+00	.7333E-03
.0879	1.02157E-04			
	INNER	.7933E+05	.1423E+00	.9477E-03
	OUTER	.6559E+05	.1407E+00	.9263E-03
.1746	1.53309E-04			
	INNER	.9829E+05	.1560E+00	.1138E-02
	OUTER	.8126E+05	.1540E+00	.1109E-02
.2898	2.04512E-04			
	INNER	.1148E+06	.1685E+00	.1327E-02
	OUTER	.9490E+05	.1661E+00	.1291E-02
.4356	2.55768E-04			
	INNER	.1298E+06	.1802E+00	.1519E-02
	OUTER	.1073E+06	.1776E+00	.1475E-02
.6146	3.07081E-04			
	INNER	.1437E+06	.1915E+00	.1714E-02
	OUTER	.1188E+06	.1886E+00	.1662E-02
.8295	3.58452E-04			
	INNER	.1569E+06	.2024E+00	.1914E-02
	OUTER	.1297E+06	.1992E+00	.1855E-02
1.0833	4.09884E-04			
	INNER	.1695E+06	.2131E+00	.2120E-02
	OUTER	.1401E+06	.2096E+00	.2052E-02
1.3793	4.61378E-04			
	INNER	.1816E+06	.2235E+00	.2332E-02
	OUTER	.1502E+06	.2198E+00	.2255E-02
1.7209	5.12938E-04			
	INNER	.1934E+06	.2337E+00	.2549E-02
	OUTER	.1599E+06	.2298E+00	.2464E-02
2.1115	5.64565E-04			
	INNER	.2049E+06	.2438E+00	.2773E-02
	OUTER	.1694E+06	.2397E+00	.2679E-02
2.5548	6.16262E-04			
	INNER	.2161E+06	.2538E+00	.3004E-02
	OUTER	.1786E+06	.2494E+00	.2901E-02
3.0546	6.68031E-04			
	INNER	.2271E+06	.2637E+00	.3241E-02
	OUTER	.1877E+06	.2591E+00	.3128E-02
3.6148	7.19874E-04			
	INNER	.2379E+06	.2735E+00	.3484E-02
	OUTER	.1967E+06	.2686E+00	.3362E-02
4.2397	7.71794E-04			
	INNER	.2485E+06	.2832E+00	.3735E-02
	OUTER	.2055E+06	.2781E+00	.3603E-02
4.9333	8.23794E-04			
	INNER	.2590E+06	.2929E+00	.3992E-02
	OUTER	.2141E+06	.2876E+00	.3849E-02
5.70	8.75875E-04			
	INNER	.2694E+06	.3025E+00	.4256E-02
	OUTER	.2227E+06	.2969E+00	.4103E-02

COMPUTER OUTPUT III (CONTINUED)

6.5445	9.28040E-04			
	INNER	.2796E+06	.3120E+00	.4526E-02
	OUTER	.2312E+06	.3063E+00	.4363E-02
7.4712	9.80292E-04			
	INNER	.2898E+06	.3215E+00	.4804E-02
	OUTER	.2396E+06	.3156E+00	.4629E-02
8.485	.001			
	INNER	.2999E+06	.3310E+00	.5089E-02
	OUTER	.2480E+06	.3248E+00	.4903E-02
9.5909	.0011			
	INNER	.3099E+06	.3404E+00	.5380E-02
	OUTER	.2562E+06	.3341E+00	.5182E-02
10.7939	.0011			
	INNER	.3199E+06	.3498E+00	.5678E-02
	OUTER	.2645E+06	.3433E+00	.5469E-02
12.0993	.0012			
	INNER	.3297E+06	.3592E+00	.5984E-02
	OUTER	.2726E+06	.3524E+00	.5762E-02
13.5124	.0012			
	INNER	.3396E+06	.3686E+00	.6296E-02
	OUTER	.2808E+06	.3616E+00	.6062E-02
15.0388	.0013			
	INNER	.3494E+06	.3779E+00	.6615E-02
	OUTER	.2888E+06	.3707E+00	.6368E-02
16.6841	.0013			
	INNER	.3591E+06	.3872E+00	.6942E-02
	OUTER	.2969E+06	.3798E+00	.6682E-02
18.4542	.0014			
	INNER	.3688E+06	.3965E+00	.7275E-02
	OUTER	.3049E+06	.3889E+00	.7002E-02
20.355	.0015			
	INNER	.3785E+06	.4058E+00	.7615E-02
	OUTER	.3129E+06	.3980E+00	.7328E-02
22.3927	.0015			
	INNER	.3881E+06	.4151E+00	.7962E-02
	OUTER	.3209E+06	.4071E+00	.7662E-02
24.5735	.0016			
	INNER	.3977E+06	.4244E+00	.8317E-02
	OUTER	.3288E+06	.4162E+00	.8002E-02
26.9041	.0016			
	INNER	.4073E+06	.4337E+00	.8678E-02
	OUTER	.3367E+06	.4252E+00	.8349E-02
29.3908	.0017			
	INNER	.4169E+06	.4429E+00	.9047E-02
	OUTER	.3447E+06	.4343E+00	.8703E-02
32.0407	.0017			
	INNER	.4264E+06	.4522E+00	.9422E-02
	OUTER	.3525E+06	.4433E+00	.9063E-02
34.8605	.0018			
	INNER	.4359E+06	.4614E+00	.9805E-02
	OUTER	.3604E+06	.4524E+00	.9430E-02
37.8574	.0018			
	INNER	.4454E+06	.4707E+00	.1019E-01
	OUTER	.3683E+06	.4614E+00	.9804E-02
41.0388	.0019			
	INNER	.4549E+06	.4799E+00	.1059E-01
	OUTER	.3761E+06	.4705E+00	.1018E-01
44.412	.0019			
	INNER	.4644E+06	.4892E+00	.1099E-01

COMPUTER OUTPUT IV

INN. RACE DIA., BALL DIA., DIA. CLEARANCE, B, NO. OF BALLS AND INCREMENT
IN ALFA, MAX HERTZ LIMIT

.3401 .0937 8.00000E-04 .04 8
.0046 460000.00

SM, ABJ 2.191 120439.37

THRUST LOAD, AXL. DSPL.

RACE, HERTZ PRESSURE, MIN. ANGLE AND LAND HEIGHT

.4319	1.93546E-05			
	INNER	.6632E+05	.5308E+00	.1290E-01
	OUTER	.5434E+05	.5288E+00	.1280E-01
1.2455	3.88001E-05			
	INNER	.9412E+05	.5606E+00	.1435E-01
	OUTER	.7711E+05	.5578E+00	.1421E-01
2.3326	5.83378E-05			
	INNER	.1157E+06	.5848E+00	.1558E-01
	OUTER	.9477E+05	.5813E+00	.1540E-01
3.6605	7.79693E-05			
	INNER	.1340E+06	.6061E+00	.1670E-01
	OUTER	.1098E+06	.6021E+00	.1648E-01
5.214	9.76961E-05			
	INNER	.1504E+06	.6257E+00	.1776E-01
	OUTER	.1232E+06	.6211E+00	.1751E-01
6.9849	1.17520E-04			
	INNER	.1653E+06	.6439E+00	.1877E-01
	OUTER	.1354E+06	.6388E+00	.1849E-01
8.9692	1.37442E-04			
	INNER	.1791E+06	.6612E+00	.1976E-01
	OUTER	.1468E+06	.6557E+00	.1944E-01
11.1656	1.57464E-04			
	INNER	.1922E+06	.6778E+00	.2072E-01
	OUTER	.1574E+06	.6719E+00	.2038E-01
13.574	1.77587E-04			
	INNER	.2045E+06	.6938E+00	.2167E-01
	OUTER	.1676E+06	.6875E+00	.2129E-01
16.1959	1.97814E-04			
	INNER	.2163E+06	.7093E+00	.2261E-01
	OUTER	.1772E+06	.7026E+00	.2220E-01
19.0335	2.18146E-04			
	INNER	.2277E+06	.7243E+00	.2354E-01
	OUTER	.1865E+06	.7173E+00	.2310E-01
22.0396	2.38584E-04			
	INNER	.2386E+06	.7391E+00	.2446E-01
	OUTER	.1955E+06	.7317E+00	.2399E-01
25.3679	2.59130E-04			
	INNER	.2492E+06	.7535E+00	.2538E-01
	OUTER	.2042E+06	.7458E+00	.2488E-01
28.8722	2.79787E-04			
	INNER	.2595E+06	.7677E+00	.2630E-01
	OUTER	.2126E+06	.7596E+00	.2577E-01
32.6069	3.00555E-04			
	INNER	.2696E+06	.7817E+00	.2721E-01
	OUTER	.2209E+06	.7732E+00	.2666E-01
36.5766	3.21437E-04			
	INNER	.2794E+06	.7954E+00	.2813E-01
	OUTER	.2289E+06	.7867E+00	.2754E-01
40.7866	3.42434E-04			
	INNER	.2889E+06	.8090E+00	.2904E-01
	OUTER	.2368E+06	.8000E+00	.2843E-01
45.2419	3.63549E-04			
	INNER	.2984E+06	.8225E+00	.2996E-01
	OUTER	.2445E+06	.8131E+00	.2932E-01

COMPUTER OUTPUT IV (CONTINUED)

49.9483	3.84782E-04			
	INNER	.3076E+06	.8358E+00	.3088E-01
	OUTER	.2520E+06	.8261E+00	.3021E-01
54.9115	4.06137E-04			
	INNER	.3167E+06	.8489E+00	.3180E-01
	OUTER	.2595E+06	.8389E+00	.3110E-01
60.1376	4.27615E-04			
	INNER	.3256E+06	.8620E+00	.3273E-01
	OUTER	.2668E+06	.8517E+00	.3200E-01
65.6329	4.49217E-04			
	INNER	.3344E+06	.8750E+00	.3366E-01
	OUTER	.2740E+06	.8644E+00	.3289E-01
71.4039	4.70947E-04			
	INNER	.3432E+06	.8879E+00	.3459E-01
	OUTER	.2812E+06	.8769E+00	.3380E-01
77.4574	4.92806E-04			
	INNER	.3518E+06	.9007E+00	.3552E-01
	OUTER	.2882E+06	.8894E+00	.3470E-01
83.8003	5.14795E-04			
	INNER	.3603E+06	.9134E+00	.3646E-01
	OUTER	.2952E+06	.9019E+00	.3561E-01
90.4398	5.36919E-04			
	INNER	.3687E+06	.9261E+00	.3741E-01
	OUTER	.3021E+06	.9142E+00	.3653E-01
97.3831	5.59177E-04			
	INNER	.3770E+06	.9387E+00	.3836E-01
	OUTER	.3089E+06	.9266E+00	.3744E-01
104.638	5.81573E-04			
	INNER	.3853E+06	.9513E+00	.3931E-01
	OUTER	.3157E+06	.9388E+00	.3837E-01
112.2121	6.04109E-04			
	INNER	.3935E+06	.9638E+00	.4027E-01
	OUTER	.3224E+06	.9510E+00	.3930E-01
120.1135	6.26787E-04			
	INNER	.4016E+06	.9763E+00	.4124E-01
	OUTER	.3290E+06	.9632E+00	.4023E-01
128.3505	6.49610E-04			
	INNER	.4097E+06	.9887E+00	.4221E-01
	OUTER	.3357E+06	.9754E+00	.4117E-01
136.9313	6.72579E-04			
	INNER	.4177E+06	.1001E+01	.4319E-01
	OUTER	.3422E+06	.9875E+00	.4212E-01
145.8647	6.95698E-04			
	INNER	.4256E+06	.1014E+01	.4417E-01
	OUTER	.3488E+06	.9996E+00	.4307E-01
155.1595	7.18908E-04			
	INNER	.4336E+06	.1026E+01	.4516E-01
	OUTER	.3552E+06	.1012E+01	.4402E-01
164.8249	7.42393E-04			
	INNER	.4415E+06	.1038E+01	.4616E-01
	OUTER	.3617E+06	.1024E+01	.4499E-01
174.8701	7.65974E-04			
	INNER	.4493E+06	.1051E+01	.4716E-01
	OUTER	.3681E+06	.1036E+01	.4596E-01
185.3047	7.89714E-04			
	INNER	.4571E+06	.1063E+01	.4817E-01
	OUTER	.3745E+06	.1048E+01	.4693E-01
196.1385	8.13617E-04			
	INNER	.4649E+06	.1075E+01	.4918E-01

COMPUTER OUTPUT V

AXLOD 15:27 CY FRI 04/24/70

IN PART2

? 0.340075, 0.09375, 0.00080, 0.1178, 8, 0.0046

? 460000.

INN. RACE DIA., BALL DIA., DIA. CLEARANCE, B, NO. OF BALLS AND INCREMENT
IN ALFA

.3401	.0937	8.00000E-04	.1178	8
.0046				

SM, ABJ 2.7669 428916.72

THRUST LOAD, AXL. DSPL.

	RACE , HERTZ	PRESSURE, MAX.	ANGLE	AND LAND HEIGHT
.3767	5.27779E-05			
	INNER	.9367E+05	.3193E+00	.4740E-02
	OUTER	.7746E+05	.3174E+00	.4684E-02
1.0984	1.05693E-04			
	INNER	.1331E+06	.3428E+00	.5455E-02
	OUTER	.1101E+06	.3401E+00	.5370E-02
2.0796	1.58747E-04			
	INNER	.1638E+06	.3621E+00	.6080E-02
	OUTER	.1354E+06	.3588E+00	.5969E-02
3.2984	2.11945E-04			
	INNER	.1900E+06	.3793E+00	.6663E-02
	OUTER	.1571E+06	.3754E+00	.6529E-02
4.7473	2.65287E-04			
	INNER	.2134E+06	.3951E+00	.7224E-02
	OUTER	.1765E+06	.3908E+00	.7067E-02
6.4246	3.18778E-04			
	INNER	.2349E+06	.4100E+00	.7772E-02
	OUTER	.1942E+06	.4052E+00	.7593E-02
8.3323	3.72420E-04			
	INNER	.2549E+06	.4243E+00	.8312E-02
	OUTER	.2108E+06	.4191E+00	.8112E-02
10.4741	4.26216E-04			
	INNER	.2738E+06	.4380E+00	.8848E-02
	OUTER	.2264E+06	.4323E+00	.8626E-02
12.8552	4.80169E-04			
	INNER	.2917E+06	.4512E+00	.9382E-02
	OUTER	.2412E+06	.4452E+00	.9139E-02

COMPUTER OUTPUT V (CONTINUED)

15.4818	5.34282E-04			
	INNER	.3089E+06	.4641E+00	.9917E-02
	OUTER	.2554E+06	.4578E+00	.9652E-02
18.361	5.88558E-04			
	INNER	.3255E+06	.4767E+00	.1045E-01
	OUTER	.2691E+06	.4700E+00	.1017E-01
21.5004	6.43000E-04			
	INNER	.3415E+06	.4891E+00	.1099E-01
	OUTER	.2824E+06	.4820E+00	.1068E-01
24.9031	6.97611E-04			
	INNER	.3570E+06	.5012E+00	.1153E-01
	OUTER	.2952E+06	.4938E+00	.1120E-01
28.5927	7.52394E-04			
	INNER	.3722E+06	.5131E+00	.1207E-01
	OUTER	.3077E+06	.5055E+00	.1172E-01
32.5632	8.07353E-04			
	INNER	.3869E+06	.5249E+00	.1262E-01
	OUTER	.3200E+06	.5169E+00	.1225E-01
36.8291	8.62490E-04			
	INNER	.4014E+06	.5366E+00	.1317E-01
	OUTER	.3319E+06	.5283E+00	.1278E-01
41.40	9.17809E-04			
	INNER	.4156E+06	.5481E+00	.1373E-01
	OUTER	.3437E+06	.5395E+00	.1331E-01
46.2861	9.73313E-04			
	INNER	.4295E+06	.5595E+00	.1429E-01
	OUTER	.3552E+06	.5506E+00	.1385E-01
51.4977	.001			
	INNER	.4433E+06	.5703E+00	.1486E-01
	OUTER	.3665E+06	.5616E+00	.1440E-01
57.0454	.0011			
	INNER	.4568E+06	.5820E+00	.1543E-01
	OUTER	.3777E+06	.5725E+00	.1495E-01
62.9403	.0011			
	INNER	.4701E+06	.5931E+00	.1601E-01

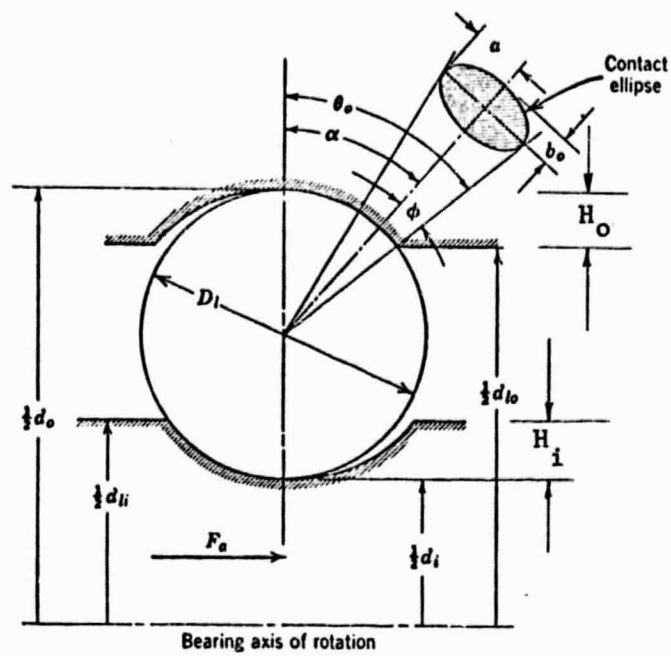


FIGURE 10. BALL RACEWAY CONTACT UNDER LIMITING THRUST LOAD

outer race, at the specified increments in α . It continues to do so until the maximum Hertz pressure at the inner race (or outer race) exceeds the limiting value specified through input, at which point it terminates further calculations. The termination of calculations is also affected if the required value of θ_0 (or θ_1) exceeds $\pi/2$.

In the computer output II and III it may be observed that for a limiting Hertz stress of 460,000 psi the load capacity of the bearing is reduced from approximately 102 pounds to 44 pounds as the parameter B, or $(f_o + f_i - 1)$ is increased from 0.04 to 0.1178, keeping all other geometrical parameters constant. Increasing B reduces ball-race conformity or the closeness of fit between ball and race groove.

Computer outputs IV and V for the same calculations are repeated for an 8-fold increase in diametral clearance. These results indicate that the reduction in conformity level (or increase in B) reduces the load carrying capacity of the bearing, whereas an increase in diametral clearance (which increases contact angle) increases the load capacity with a limit imposed by race land height. Thus, by changing the contact angle with the present size bearing, an increase in load capacity is possible without changing bearing size. It must be kept in mind, however, that increasing contact angle will also increase ball spin and heat generation in the bearing. This effect will tend to reduce the endurance life of the bearing in terms of lubricant degradation and ball wear.

RECOMMENDED PROCEDURE FOR CHOICE OF BEARINGS IN SIMILAR FUTURE APPLICATIONS

The analysis of the present PLV fan bearings has demonstrated the importance of the dynamical considerations in the choice of bearings for a similar application. At the same time, one is forced to recognize that it is not possible to outline a simple step-by-step procedure that would end in the selection of a bearing satisfying all the design requirements. As is typical of such problems the designer must consider the influence of various parameters on the outcome before arriving at the final optimum design. The next few paragraphs present a plan of analysis to arrive at such an optimum design.

It is assumed that the mass of the rotor is known. It is also assumed that Power Spectral Density (PSD) of the vibration environment to be imposed on the rotor, is known. It is desired to determine the maximum axial load that would be borne by the bearing under fairly severe conditions. Based on this estimate, the geometry of the angular contact bearing would be selected so as to avoid the brinelling of the race as well as balls over-riding the race land. To facilitate the choice of the bearing it is necessary that this load-limit be as small as possible.

Equation (A-14) relates the axial load on the bearing with the stiffness of the system, its damping, and the maximum expected amplitude of vibration on the bearing-rotor assembly. The expected amplitude of vibration, for the white-noise approximation, is in turn related to the maximum value of the PSD (W_0) resonant frequency (f_n) and the magnification factor (Q) as given by (A-13). If the axial displacement of the rotor must be kept at an absolute minimum (from the viewpoint of design limitation) then the resonant frequency of the system must be chosen past the higher end of the PSD spectrum to minimize the value of W_0 . This requires that stiffness of the system be high which would in turn require that the support system must be made very rigid. The latter requirement may be difficult to realize if the stipulated resonant frequency is of the order of 2000 HZ and over; in this case a compromise will have to be made, such as, allowing for larger amplitude-limit and perhaps even larger loads on the bearing. If, however, the required resonant frequency can be obtained with a reasonably rigid support system the reduction of the load-limit on the bearing would be easily achieved in the high-frequency end of the PSD spectrum.

On the other hand, if the axial displacement is not the limiting quantity, the load-limit on the bearing can be reduced by going to the low-frequency-end of the PSD spectrum. Below a certain level of the resonant frequency the value of W_0 will decrease. The low resonant frequency can be designed by suspending the rotor-bearing system in a soft suspension system (e.g. five springs in the present PLV fan bearings) such that the preloaded bearing acts essentially as a rigid member. For the suspension system use can be made of thick elastomeric packing material which would provide high damping factor as well. It is, of course, necessary that the "collapse-

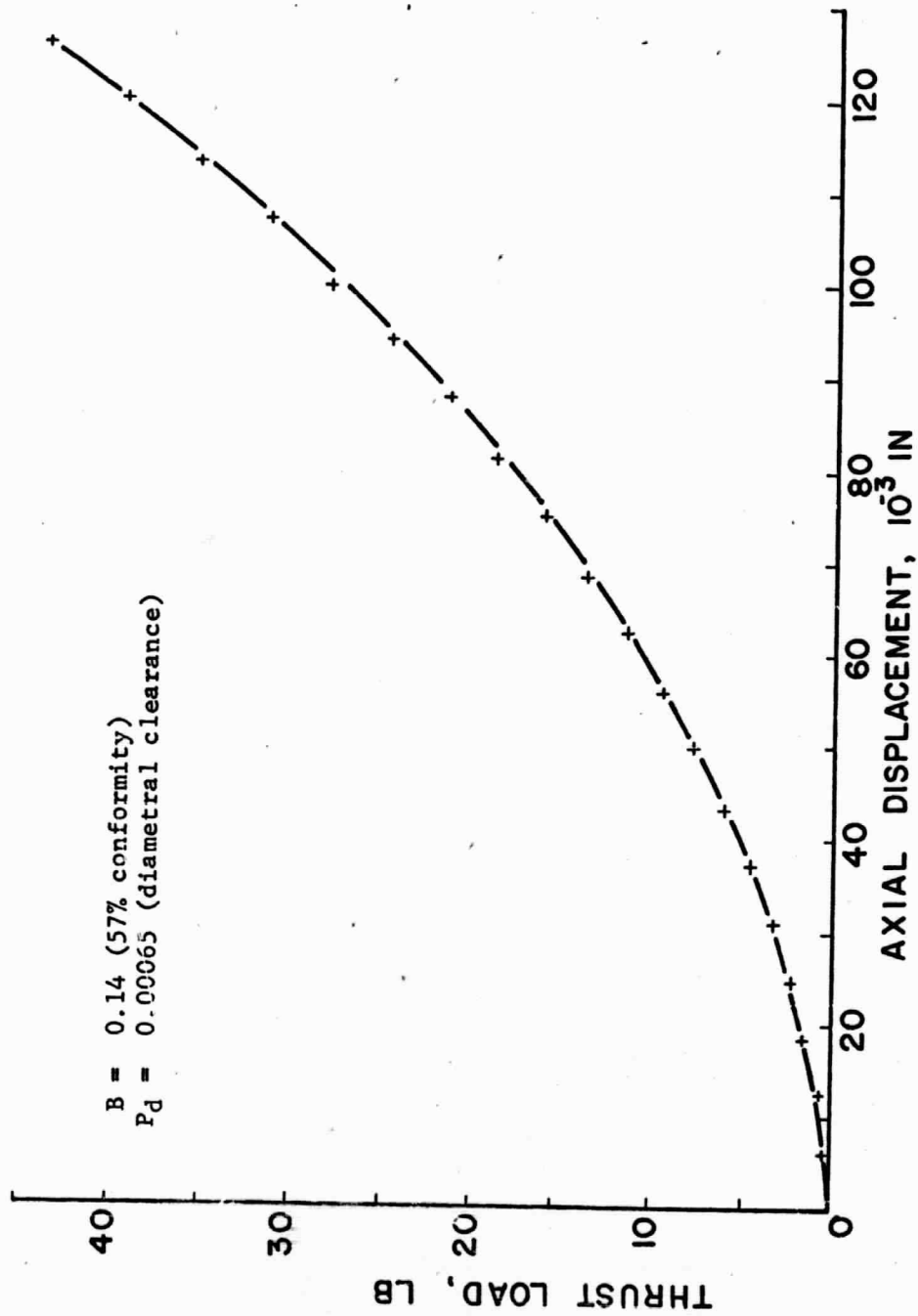


FIGURE 9. LOAD DEFLECTION CURVE FOR PLV FAN BEARING

COMPUTER OUTPUT II

AXL0D 16:07 CY FRI 04/24/70

IN PART2

? 0.340075, 0.09375, 0.0001, 0.04, 3, 0.0046, 460000.

INN. RACE DIA., BALL DIA., DIA. CLEARANCE, B, NO. OF BALLS AND INCREMENT
IN ALFA, MAX HERTZ LIMIT.3401 .0937 1.00000E-04 .04 8
.0046 460000.00

SM, ABJ 2.1909 120441.83

THRUST LOAD, AXL. DSFL.

	RACE, HERTZ	PRESSURE, MIN.	ANGLE	AND LAND HEIGHT
.0303	1.74965E-05			
	INNER	.3812E+05	.2026E+00	.1918E-02
	OUTER	.3123E+05	.2015E+00	.1896E-02
.2792	7.01533E-05			
	INNER	.7790E+05	.2525E+00	.2972E-02
	OUTER	.6382E+05	.2501E+00	.2917E-02
.7392	1.23078E-04			
	INNER	.1052E+06	.2911E+00	.3944E-02
	OUTER	.8619E+05	.2879E+00	.3858E-02
1.4336	1.76293E-04			
	INNER	.1283E+06	.3259E+00	.4935E-02
	OUTER	.1051E+06	.3220E+00	.4818E-02
2.3985	2.29821E-04			
	INNER	.1491E+06	.3588E+00	.5969E-02
	OUTER	.1222E+06	.3542E+00	.5819E-02
3.6761	2.83686E-04			
	INNER	.1686E+06	.3904E+00	.7053E-02
	OUTER	.1381E+06	.3852E+00	.6869E-02
5.3131	3.37912E-04			
	INNER	.1871E+06	.4212E+00	.8193E-02
	OUTER	.1533E+06	.4154E+00	.7974E-02
7.3607	3.92522E-04			
	INNER	.2050E+06	.4514E+00	.9391E-02
	OUTER	.1680E+06	.4451E+00	.9134E-02
9.8737	4.47542E-04			
	INNER	.2224E+06	.4813E+00	.1065E-01
	OUTER	.1822E+06	.4744E+00	.1035E-01
12.9116	5.02998E-04			
	INNER	.2394E+06	.5108E+00	.1197E-01
	OUTER	.1961E+06	.5034E+00	.1163E-01

COMPUTER OUTPUT II (CONTINUED)

14.0517	5.21585E-04			
	INNER	.2450E+06	.5206E+00	.1242E-01
	OUTER	.2007E+06	.5130E+00	.1207E-01
15.2595	5.40224E-04			
	INNER	.2506E+06	.5304E+00	.1288E-01
	OUTER	.2053E+06	.5226E+00	.1251E-01
16.5377	5.58917E-04			
	INNER	.2562E+06	.5402E+00	.1335E-01
	OUTER	.2099E+06	.5322E+00	.1297E-01
20.8201	6.15326E-04			
	INNER	.2727E+06	.5694E+00	.1479E-01
	OUTER	.2234E+06	.5609E+00	.1436E-01
25.8313	6.72252E-04			
	INNER	.2891E+06	.5985E+00	.1630E-01
	OUTER	.2368E+06	.5895E+00	.1582E-01
31.6488	7.29726E-04			
	INNER	.3053E+06	.6276E+00	.1787E-01
	OUTER	.2501E+06	.6180E+00	.1734E-01
38.3552	7.87778E-04			
	INNER	.3215E+06	.6567E+00	.1950E-01
	OUTER	.2634E+06	.6465E+00	.1892E-01
46.0354	8.46438E-04			
	INNER	.3376E+06	.6858E+00	.2120E-01
	OUTER	.2766E+06	.6751E+00	.2056E-01
54.792	9.05739E-04			
	INNER	.3537E+06	.7150E+00	.2296E-01
	OUTER	.2898E+06	.7036E+00	.2227E-01
64.7157	9.65715E-04			
	INNER	.3698E+06	.7442E+00	.2478E-01
	OUTER	.3030E+06	.7323E+00	.2403E-01
75.9155	.001			
	INNER	.3859E+06	.7735E+00	.2667E-01
	OUTER	.3162E+06	.7610E+00	.2586E-01
88.5039	.0011			
	INNER	.4020E+06	.8029E+00	.2863E-01
	OUTER	.3294E+06	.7898E+00	.2775E-01
102.6009	.0012			
	INNER	.4182E+06	.8325E+00	.3065E-01

USED 60.00 UNITS

load" of the soft suspension system be at least as high as the maximum load capacity of the bearing.

Once the load limit of the bearing has been arrived at, in the above manner, the design parameter for the angular contact bearing can be established by the computer program described in the preceding section. To guard against brinelling it is recommended that maximum Hertz pressure be kept below 460,000 psi under all conditions. This would then provide a limiting criteria for the geometrical parameters of the bearings to be selected.

CONCLUSIONS AND RECOMMENDATIONS FOR FUTURE WORK

The following conclusions have been drawn from the analysis of the PLV fan bearing problem:

- (1) The bearing failure mode is vibration induced race brinelling, the damaging loads occurring in the axial direction.
- (2) Maximum bearing load can be reduced by decreasing the natural frequency of the rotor-bearing-preload spring system. This can be accomplished by mounting preload springs in series at both bearing supports on the rotor.
- (3) A computer program, written to calculate maximum load capacity based on brinelling mode of failure, has demonstrated that bearing load capacity can be increased by altering contact angle and ball-race conformity.
- (4) A system has been established for selection of ball bearings for similar rotor support problems in vibration environment (assuming the Power Spectral Density is given).

FUTURE WORK

It was found that the criterion for brinelling damage in ball bearings is based on an arbitrary maximum Hertz stress level. This level has

been arrived at in bearing technology by static load tests on ball-race configurations. For applications where minimum bearing size is required a more accurate criterion should be established. We recommend that selected rolling contact bearings be subjected to vibration evaluations in which the maximum bearing load as determined from the analysis in this summary be varied over a range selected to cover nonbrinelling and brinelling levels. The extent of damage would then be evaluated on the basis of noise level during rotation under steady state load.

APPENDIX A

ANALYSIS OF FAN BEARING LOADS FROM RANDOM VIBRATION